

**“A 3-Dimensional co-culture model of Inflammatory Bowel Disease for therapy
screening”**

Submitted by

PARASKEVI TSELEKOUNI

Supervisors: Derek H. Rosenzweig, Peter L. Lakatos

A thesis submitted to McGill University in partial fulfillment of the requirements of the degree
of MASTER OF SCIENCE (M.Sc.)

Dept. of Experimental Surgery- Surgical Innovation,

Faculty of Medicine and Health Sciences

McGill University

Montreal, Quebec, Canada



© Paraskevi Tselekouni, July 2023

TABLE OF CONTENTS

Abstract.....	5
Resume	6
Acknowledgments	8
List of Figures.....	9
Abbreviations	11
CHAPTER 1: INTRODUCTION	14
1.1 IBD Epidemiology	14
1.2 IBD Pathophysiology	17
1.2.1 Genetic factors	17
1.2.2 Intestinal microbiota	17
1.2.3 Environmental factors	18
1.2.4 Immunological factors	19
1.3 Clinical Features of IBD	23
1.4 Treatment in IBD	25
1.4.1 “Treat-to-target” strategy	25
1.4.2 Therapeutic options	26
1.4.2.a Aminosalicylates	26
1.4.2.b Corticosteroids	26
1.4.2.c Immunomodulators	27
1.4.2.d Biologic anti-TNF therapy	28
1.4.2.e Biologic Anti-IL-12/23 Therapy	28

1.4.2.f	Biologic Anti-integrin therapy	29
1.4.2.g	Small molecules- JAK inhibitors	30
1.4.2.h	Surgical Management	31
1.4.3	Novel treatment	31
1.5	Research Tools for personalized medicine	33
1.5.1	Animal models	34
1.5.2	2D models	35
1.5.3	3D models	36
1.5.4	Comparison of the existing research tools	38
CHAPTER 2: METHODS		39
2.1	Objective of the Study and clinical significance	39
2.2	Objective 1- Generation of 3D culture models	40
2.2.1	Materials that were used	40
2.2.1.a	HT-29 cell line	40
2.2.1.b	IRM-90 cell line	42
2.2.1.c	Alginate-Gelatin Hydrogel	45
2.2.1.d	Cross-linking agent and culture medium	46
2.2.2	3D Modeling Technique	47
2.2.3	Evaluation Assays of the 3D single culture and co-culture system	50
2.3	Objective 2- Modeling IBD with the 3D co-culture system	53
2.3.1	Factors that induce inflammation	53
2.3.2	Inducing and suppressing inflammation – experimental process	55

2.3.3 Evaluation of model response to inflammation and anti-inflammatory factors	56
2.4 Statistical analysis	57
CHAPTER 3: RESULTS	57
3.1 3D Model Characterization	57
3.2 Cell metabolic activity	59
3.3 Cell viability	60
3.4 Cell proliferation	64
3.5 Cytokine expression	65
CHAPTER 4: DISCUSSION	69
4.1 Cell types and hydrogel type	70
4.2 IBD Modeling using our 3D co-culture system	72
4.3 Limitations	73
CHAPTER 5: CONCLUSION AND FUTURE APPROACH	75
BIBLIOGRAPHY.....	76

ABSTRACT

Inflammatory bowel disease (IBD) is a chronic intestinal disorder affecting patient survival and Quality of Life. Surprisingly, Canada has one of the highest prevalence of inflammatory bowel disease worldwide, leading to a high economic burden. Although there are classic treatment options and newer therapeutics, we don't know in advance which therapeutic agent is appropriate for each patient. In addition, some patients don't respond to the existing therapy, indicating a need for improved treatments and personalized medicine. Studies use animal models or 2-Dimension culture models, but these research tools have limitations and don't recapitulate human disease. Therefore, more clinically relevant models are more appropriate for mechanistic studies and screening of new therapeutic options. This study generated a 3-Dimensional co-culture system, including the HT-29 intestinal epithelial cell line and IRM-90 fibroblast cell line, seeded in Alginate-Gelatin Hydrogel. Our research tool was evaluated, and the results showed that the 3D co-culture system supports cell viability, cell metabolic activity, and cell proliferation. Then, modeling IBD was the next step in our study. We used Lipopolysaccharide (LPS) to induce inflammation, and then we added dexamethasone to the LPS-treated models to suppress inflammation. We evaluated our model response by measuring the culture medium's TNF α and IL-1 β cytokine levels. Our results showed that the 3D co-culture model responded to the inflammatory factor by expressing higher levels of the above cytokines compared to the control group. Also, the cytokine expression was decreased after dexamethasone use in the LPS-treated models. Our results suggest that our 3D co-culture system is responsive to inflammation and anti-inflammatory therapeutics. Further studies can be done using IBD-patient-derived intestinal cells overlaid on a fibroblast basement membrane.

RÉSUMÉ

La maladie inflammatoire chronique de l'intestine (MICI) est un trouble intestinal qui affecte la survie et la qualité de vie des patients. Étonnamment, le Canada a l'une des prévalences les plus élevées de maladies inflammatoires de l'intestin au monde, ce qui entraîne un lourd fardeau économique. Bien qu'il existe des options de traitement classiques et des thérapies plus récentes, nous ne savons pas à l'avance quel agent thérapeutique est approprié pour chaque patient. De plus, certains patients ne répondent pas au traitement existant, ce qui indique un besoin de thérapies améliorées et de médecine personnalisée. Il existe des études utilisant des modèles animaux ou des modèles de culture à 2 dimensions, mais ces outils de recherche ont des limites et ne récapitulent pas la maladie humaine. Par conséquent, des modèles plus pertinents sur le plan clinique sont plus appropriés pour les études mécanistes et le criblage de nouvelles options thérapeutiques. Dans cette étude, nous avons généré un système de co-culture tridimensionnelle, comprenant la lignée cellulaire épithéliale intestinale HT-29 et la lignée cellulaire de fibroblastes IRM-90,ensemencées dans de l'hydrogel d'alginate-gélatine. Notre outil de recherche a été évalué et les résultats ont montré que le système de co-culture 3D soutient la viabilité cellulaire, l'activité métabolique cellulaire et la prolifération cellulaire. Ensuite, la modélisation des MICI a été la prochaine étape de notre étude. Nous avons utilisé le lipopolysaccharide (LPS) pour induire l'inflammation, puis nous avons ajouté de la dexaméthasone aux modèles traités au LPS pour supprimer l'inflammation. Nous avons évalué la réponse de notre modèle en mesurant les taux de cytokines $\text{TNF}\alpha$ et $\text{IL-1}\beta$ dans le milieu de culture. Nos résultats ont montré que le modèle de co-culture 3D répondait au facteur inflammatoire en exprimant des niveaux plus élevés des cytokines ci-dessus par rapport au groupe témoin. De plus,

après l'utilisation de la dexaméthasone dans les modèles traités au LPS, l'expression des cytokines a diminué. Nos résultats suggèrent que notre système de co-culture 3D est sensible à l'inflammation et aux thérapeutiques anti-inflammatoires. D'autres études pour la modélisation des MICI peuvent être réalisées en utilisant des cellules intestinales dérivées de patients atteints des MICI superposées sur la membrane basale des fibroblastes.

ACKNOWLEDGEMENTS

Working with Dr. Derek Hadar Rosenzweig and Dr. Peter Lazlo Lakatos has been a pleasure and privilege since September 2021. I am incredibly thankful for their guidance, patience, and support.

I want to thank Derek for his calm, friendly approach and targeted comments on my work. Thanks for pushing me to look at the bigger picture and learn new experimental techniques. I would also like to thank Peter, my fellowship director, for his support and understanding while I was trying to synchronize my research work and my fellowship duties. I would also like to thank Dr. Jacques Lapointe, my research advisory committee chair, for his time and thoughtful feedback.

This work could not have been possible without the support and counsel of many talented students and post-doctoral fellows. To Ateeque Siddique, for his helpful advice and the many conversations while waiting for the experiments' next step; to Matthew Mannarino, for his instructions concerning the ELISA assay; to Mansoureh Mohseni for her help and guidance during the experiments; to Gargi Goel, Eleane Hamburger, and Laura Bouret for their everyday help and company in the laboratory. Special thanks to Dr. Rita Kohen, a precious collaborator at the laboratory and in my fellowship program. And, of course, I am so grateful and blessed for the support and friendship of all the lab members.

Lastly, I would like to thank my husband and daughter for giving me courage and happiness during the training process.

LIST OF FIGURES

Figure 1 – Four Gastrointestinal (GI) Layers	21
Figure 2 – Cell interaction in IBD pathogenesis	22
Figure 3 – IBD pathogenesis	23
Figure 4 – Types of research tools	33
Figure 5 – electronic microscopy image of 2-Dimensional HT-29 cell culture	42
Figure 6 – electronic microscope image of 2D mCherry IRM-90 Fibroblast culture...	45
Figure 7 – Generation procedure of 3D cell culture models (schematic illustration)...	49
Figure 8 – 3D cell culture models	49
Figure 9 – culture plate of 3D cell culture systems	50
Figure 10 – electronic microscope image of 3D HT-29 cell culture model	58
Figure 11 – electronic microscope image of 3D co-culture model	58
Figure 12 – Metabolic activity of 3D culture models on Days 1,3 & 7	60
Figure 13 – fluorescence microscope image of 3D HT-29 model on Days 1,3 & 7	61
Figure 14 – fluorescence microscope image of 3D IRM-90 model on Days 1,3 & 7	61
Figure 15 – fluorescence microscope image of 3D co-culture models on Day 7	62
Figure 16 – Cell viability of 3D single cell culture models on Days 1,3 & 7.....	63
Figure 17 – Cell viability of 3D single cell and co-culture models on Day 7.....	64
Figure 18 – Cell proliferation of 3D models	65

Figure 19 – Per fold cell number increase of 3D models66

Figure 20 –TNF α concentration after LPS Treatment and after
Dexamethasone Treatment68

Figure 21 – IL-1 β concentration after LPS Treatment and after
Dexamethasone Treatment68

ABBREVIATIONS

2D: 2- Dimensional

3D: 3-Dimensional

5-ASA: 5-aminosalicylic acid

A1G7: Alginate (1% v/v)- Gelatin (7% v/v)

ATG16L1 gene: autophagy-related 16-like 1 gene

CD: Crohn's Disease

CDAI score: Crohn's Disease Activity Index (score)

DMEM: Dulbecco's Modified Eagle Medium

DMSO: Dimethyl Sulfoxide

DNA: Deoxyribonucleic acid

DsRed: Discosoma sp. Coral

DSS: dextran sulfate sodium

ECM: Extracellular Matrix

EGF: Epidermal Growth Factor

EIMs: Extra-intestinal manifestations

ELISA: Enzyme-Linked Immunosorbent Assay

FMT: Fecal microbiota transplant

FBS: Fetal Bovine Serum

GI: Gastrointestinal

IBD: Inflammatory Bowel Disease

IBD-I: Indeterminate Inflammatory Bowel Disease

IL: Interleukin

ISCs: Intestinal Stem Cells

JAK inhibitors: Janus kinase inhibitors

LOR: Loss of Response

LPS: Lipopolysaccharide

LTA: Lipoteichoic acid

MadCAM-1: Mucosal addressing Cell Adhesion Molecule 1

NK cells: Natural-Killer cells

NOD2: Nucleotide-binding oligomerization domain 2

NSAIDs: Non-steroidal anti-inflammatory drugs

PDX: Patient-Derived Xenografts

QoL: Quality of Life

RFP: Red Fluorescent Protein

RFU: Relative Fluorescent Units

SCCAI: Simple Clinical Colitis Activity Index

SD: Standard Deviation

SES-CD: Simple Endoscopic score for Crohn's disease

STATs: Signal Transducer and Activators of Transcription

Th1: Type 1 T helper cell (type of T-lymphocytes)

Th2: Type 2 T helper cell (type of T-lymphocytes)

TGF- β : Transforming growth factor beta

TLR: Toll-like Receptor

TNBS: 2,4,6-trinitrobenzene sulfonic acid

TNF α : Tumor Necrosis Factor α

Tregs: T regulatory cells (type of T- lymphocytes)

UC: Ulcerative Colitis

CHAPTER 1

INTRODUCTION

Inflammatory Bowel Disease (IBD) is a chronic intestinal disorder that causes a major global healthcare burden, significant morbidity, and reduced quality of life. IBD symptoms include intestinal manifestations (such as abdominal pain, persistent diarrhea, rectal bleeding, unintended weight loss) and extra-intestinal manifestations (such as joint pain and deformities, skin lesions, eye disorders). IBD-related symptoms are described in detail below. The two major types of IBD are Ulcerative Colitis (UC), which is limited to the colonic mucosa, and Crohn's Disease (CD), which is transmural and may affect any segment of the Gastrointestinal (GI) tract from the mouth to the anus. There is also Indeterminate Colitis (IBD-I), a subgroup of 10-15% of IBD cases in which disease features cannot distinguish between UC and CD.¹ Finally, there is also microscopic colitis, which is characterized by normal colonic mucosa. Microscopic colitis causes intestinal inflammation detected only in pathology specimens.²

1.1 IBD Epidemiology

The first reports of IBD follow the Industrial Revolution in the Western World (1850s - 1860s).³ Many cases of "idiopathic colitis" have been reported since 1859, but the term 'Ulcerative Colitis' was used in 1875 by Dr. Wilks and Dr. Moxon, who distinguish this chronic disease from diarrheal diseases by infectious agents.⁴ In addition, Crohn's disease was first described in 1932 by Burrill Crohn, Leon Ginzburg, and Gordon Oppenheimer. They studied

a granulomatous inflammation of the terminal ileum, and they called it “regional ileitis”. Finally, the disease was named “Crohn’s disease”.³

Following the 1950s, the incidence of IBD started to increase in the so-called “Western World”, such as North America and Europe.³ The end of the 20th century is combined with the onset of globalization and industrialization for countries in Asia, the Middle East, and South America. This phenomenon resulted in urbanization and westernization of their growing population, leading to IBD epidemiology changes. A general estimation is that the incidence of UC, followed by the incidence of CD, started to increase at the turn of the 21st century, similar to the rates reported for the “Western countries” during the second half of the 20th century.³ In the meanwhile, the IBD incidence seems to have plateaued in the West.⁵ As a result, the following reported epidemiologic data at the present moment are pretty interesting. In general, the incidence and prevalence of IBD are increasing globally, although there are few epidemiological data from developing countries.⁶ Most of the studies come from Europe and North America, where IBD incidence is higher than in the rest of the world.⁵ It is estimated that 0.3% of the European population has been diagnosed with IBD, corresponding to 2.5-3 million IBD patients.⁷ Regarding the prevalence, it is estimated that CD prevalence in Europe ranges from 1.5 to 213 per 100,000 and the UC prevalence ranges from 2.4 to 294 per 100,000.⁷ In North America, the estimated pooled prevalence is 0.3% in the 21st century, and it is estimated to reach 0.5-0.6% the next decade, meaning a number of approximately 2.2 million IBD patients.^{8,9}

Regarding the epidemiologic data from Canada, the reported prevalence of IBD is high (at 725 cases per 100,000 population).¹⁰ However, the incidence rates differ across the country. According to Leddin et al., the highest annual incidence of IBD was observed in Nova Scotia (17.7/100,00 for CD and 16.7/100,000 for UC), but it decreased compared to the incidence rate before the year 2000.¹¹ Decreased incidence rates between the years 2001 and 2008

were also reported in a retrospective study in Quebec, where incidence for CD was 16.8/100,000 cases in 2008 (compared to 18.1/100,000 in 2001), and incidence for UC was 9.8/100,000 in 2008 (compared to 12.5/100,000 in 2001).¹² On the other hand, the incidence rates in the Ontario province increased between 1999 and 2008. Incidence in CD was 12.1/100,000 (20% increase), and incidence for UC was 12.1/100,000 cases (11.5% increase).¹³

The high prevalence of IBD in Canada is being accused of a high economic burden. According to one Canadian study in which many provinces participated, the annual cost of caring for IBD patients in 2018 is estimated at \$1.28 billion (roughly \$4731 per person with IBD).¹⁴ It is also mentioned that the cost of health care for IBD patients is more than double compared to non-IBD patients.¹⁴

Regarding the recently industrialized part of the world, the numbers of IBD epidemiology show a continuous increase in IBD diagnosis frequency. The constant increase in IBD incidence in China led to the rise in IBD prevalence from 12,000 cases to 266,394 cases between the years 2000 and 2010.¹⁵ High incidence rates in IBD were also observed in the last decade in other Asian countries compared to incidence rates in the past (30-50% incidence rate increase in West East, 30-40% incidence rate increase in Saudi Arabia, and 40-50% incidence rate increase in Middle East).^{16,17}

Although the total number of IBD patients is increasing worldwide, the epidemiologic data concerning patient survival have been improved due to optimization in the management of IBD patients. According to an extensive worldwide study, the age-standardized death rate decreased over the last decades from 0.61 per 100,000 to 0.51 per 100,000.¹⁸

1.2 IBD Pathophysiology

The etiology of IBD is still unknown, but many factors mentioned below contribute to the initiation and progression of intestinal inflammation. The current hypothesis is that, in genetically susceptible individuals, aggressive T-cells mediate immune response to specific antigens coming from the intestinal microbiota. This continuous immune response leads to chronic inflammation triggered by environmental factors.¹⁹

1.2.1 Genetic factors: According to numerous studies, there are 242 genetic risk loci related to IBD,²⁰ and some are specific to CD and others to UC.²¹ However, it was found that around 30 genetic loci are shared between Crohn's disease and Ulcerative Colitis.¹⁹ Interestingly, many genetic loci related to IBD were also associated with other autoimmune diseases, such as psoriasis and ankylosing Spondylitis. Nucleotide-binding oligomerization domain 2 (NOD2) was the first gene found to be related to CD. Around one-third of CD patients have a mutation in the NOD2 gene, which is associated with a more severe disease phenotype.²² Another gene, the autophagy-related 16-like 1 (ATG16L1) gene, which is expressed by intestinal epithelial cells, APCs, and various types of T-cells, is associated with Paneth cell dysfunction and abnormal Toll-like Receptor (TLR) .²³ Toll-like receptors are membrane-spanning receptors usually expressed on sentinel cells, such as macrophages and dendritic cells. TLR, in normal conditions, binds pathogen molecules and recognizes the invader starting the immune system response.

1.2.2 Intestinal Microbiota: Intestinal Microbiota plays a significant role in the pathophysiology of IBD because microbes impact the immune system in many ways and affect host metabolism and gastrointestinal development. Human Intestinal Microbiota includes 1000-5000 different species. The coexistence with the microbiota can benefit host metabolism and

gastrointestinal development, but intestinal microbiome dysbiosis has been described as the factor that triggers IBD. It has been observed that IBD occurs in bowel regions where there is high bacteria concentration, namely in the terminal ileum and colon. The inflamed bowel mucosa has been associated with dysbiosis. Dysbiosis occurs when the aggressive microbe groups (such as Proteobacteria and Fusobacterium species) expand, accompanied by a decrease in protective bacteria groups (such as Bifidobacterium species, Bacteroidetes).²⁴ Antigens from the pathogenic microbe groups interact with the intestinal cells, disrupting the intestinal epithelial barrier.¹⁹

1.2.3 Environmental factors: The high prevalence of IBD in the “Western World” and the increasing incidence of IBD in newly industrialized countries indicate the impact of urbanization, industrialization, and Western lifestyle on the pathogenesis of IBD.²⁵ Recent reviews and studies revealed that a Western diet composed of low fiber and high amounts of red meat, fat and refined sugars has a pro-inflammatory effect on the intestine of predisposed individuals. More specifically, the artificial food additives that the Western diet contains are associated with dysbiosis and, as a result, with chronic inflammation and development of IBD²⁶⁻²⁸ The ENIGMA Study, which included CD patients from East World countries with high, intermediate, and emerging incidence, observed that CD patients have been exposed to more processed food and food additives than controls.²⁹ Among the other risk factors, smoking is the most extensively studied. It is considered that cigarette smoking protects against Ulcerative Colitis,³⁰ whereas smokers are more likely to be diagnosed with Crohn’s disease in the Western World.³¹ Also, Crohn’s disease patients who smoke experience complications more frequently, whereas smoking doesn’t significantly impact Ulcerative colitis progression.³² This divergent effect of smoking on CD and UC isn’t completely understood, but it is considered that intestinal permeability, cytokine production, and clotting in the

microvasculature play a significant role.³³ Furthermore, the Hygiene Hypothesis may explain the increasing epidemiologic rates of autoimmune and allergic conditions in individuals living in industrialized regions. It is believed that limited exposure to microbes in childhood doesn't adequately prime the immune system. As a result, the immune system inappropriately attacks those individuals' organs later in life after exposure to a pathogen.³⁴ Other risk factors for developing IBD are psychological stress, oral contraceptive pills, and Non-steroidal anti-inflammatory drugs (NSAIDs) use.^{3,35}

1.2.4 Immunological factors: As mentioned above, in genetic predisposal individuals, Intestinal Microbiota alterations in combination with the environmental factors mentioned above lead to an immunological dysregulation, which characterizes IBD. The gastrointestinal tract consists of 4 layers: mucosa, submucosa, muscularis and serosa (Figure 1). Immunological dysregulation takes place in the mucosa and the submucosa. Mucosa consists of the epithelium, the basement membrane of stromal cells (fibroblasts that support the epithelial cells), and the lamina propria. Submucosa is the layer where fibroblasts are located.³⁶ In this layer, there are also vessels through which immune cells translocate from the systematic circulation to the inflammation site. Disrupting the mucosal epithelial barrier allows interaction between intestinal lumen pathogens and immune cells. This interaction results in cytokine production.³⁷ Consequently, a vicious cycle of inflammation ensues.

The inflamed IBD tissue is characterized by a network of interacting cells, including the epithelial cell and microbiota, the stromal cells, phagocytes, T-lymphocytes, and B-lymphocytes. Among the T-lymphocytes are the T-effector lymphocytes that promote inflammation and the T regulatory cells (Tregs) that control inflammation.³⁸ These cells can be either the source or the target of different cytokines that affect the intestinal mucosa.³⁹⁻⁴¹ These cytokine networks can also interfere with one another, overlap, and even sort into

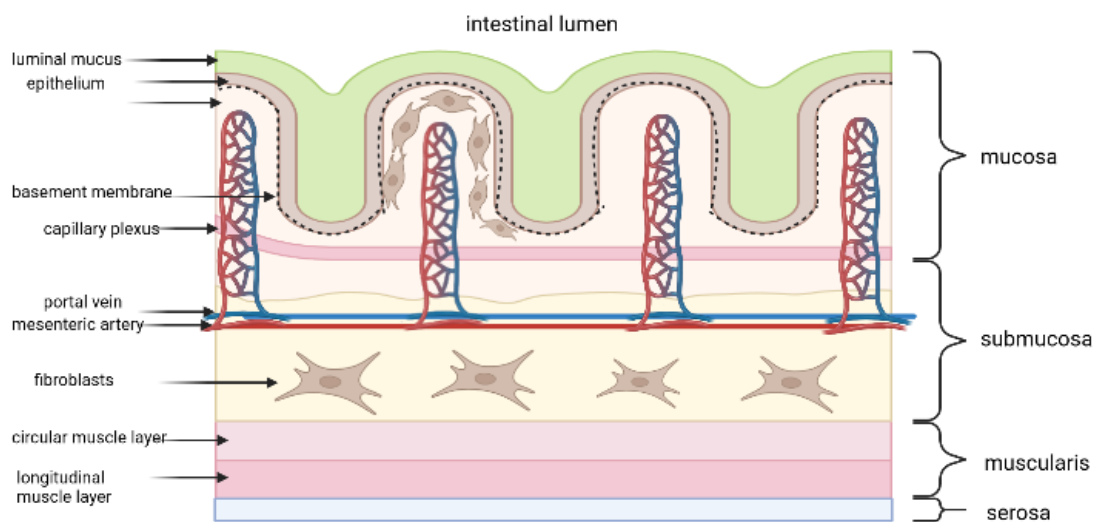
multiple cell types. That's why the Olympic rings can symbolize this cell and cytokine network (Figure 2).⁴²

The cytokine function is complex (Figure 3). In healthy conditions, cytokines such as IL-1 β , IL-5, IL-18, and IL-22 maintain homeostasis by regulating key cellular processes like cell death, proliferation, and response against pathogens.³⁷ On the other hand, the same or other cytokines, such as TNF α and IL-6, can initiate intestinal inflammation under certain circumstances, depending on the interaction between immune cells and specific pathogens that haven't yet been defined. The activated lamina propria cells can secrete a variety of cytokines, both pro-inflammatory (TNF α , IL-6, IL-12, IL-23) and anti-inflammatory cytokines (IL-10, TGF β , IL-35).³⁷

Several pro-inflammatory cytokines, such as the IL-1 family of cytokines, are involved in the progression of IBD.⁴³ According to a study of basic science, IL-1 β is expressed from IBD macrophages and promotes inflammation.⁴⁴ According to Coccia et al., IL-1 β promotes inflammation by inducing cytokine IL-17, accumulating innate lymphoid cells, and differentiating T cells to Th17 lymphocytes.⁴⁵ Another example is Tumor Necrosis Factor α (TNF α), a pro-inflammatory cytokine with immunological up-regulatory activities.⁴⁶ TNF α is produced by innate immune cells (i.e., macrophages) and differentiated T cells. TNF α induces the production of other cytokines (IL-1 β , IL-6), the expression of adhesion molecules (such as TLR), and the activation of fibroblasts. Finally, TNF participates in the inhibition of apoptosis.⁴⁶ The impact of TNF α in IBD pathogenesis is evident as this cytokine level in the serum of IBD patients is associated with the clinical severity of the disease.³⁵

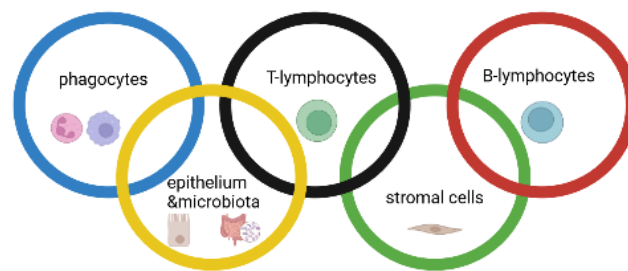
Of note, it was found that certain cytokines are related to either Crohn's disease or Ulcerative Colitis. For example, high IL-23 levels are found in CD specimens but not in UC specimens.⁴⁷ It was shown that IL-23 can induce the production of IFN- γ , IL-17, GM-CSF and promote Th1 activation.^{42,47} Subsequently, CD is characterized as a Th1-driven response. On the other

hand, UC specimens -compared to CD specimens- had high levels of IL-5 and IL-13, which are cytokines related to Th2 activation.⁴⁷ Subsequently, it is believed that UC is a Th2-driven response.^{37,47}



Created in BioRender.com 

Figure 1- GI layers. Image created in BioRender.com. All gastrointestinal tract segments are divided into four layers: the mucosa, the submucosa, the muscularis mucosa, and the serosa. Mucosa and submucosa consist of components that take part in immunological dysregulation.



Created in BioRender.com 

Figure 2- Cell network in IBD pathogenesis: different types of cells are involved in IBD pathogenesis. These cell types include epithelial cells, microbiota, stromal cells, phagocytes, B- and T-lymphocytes. They interact with each other and produce a plethora of cytokines inducing inflammation.

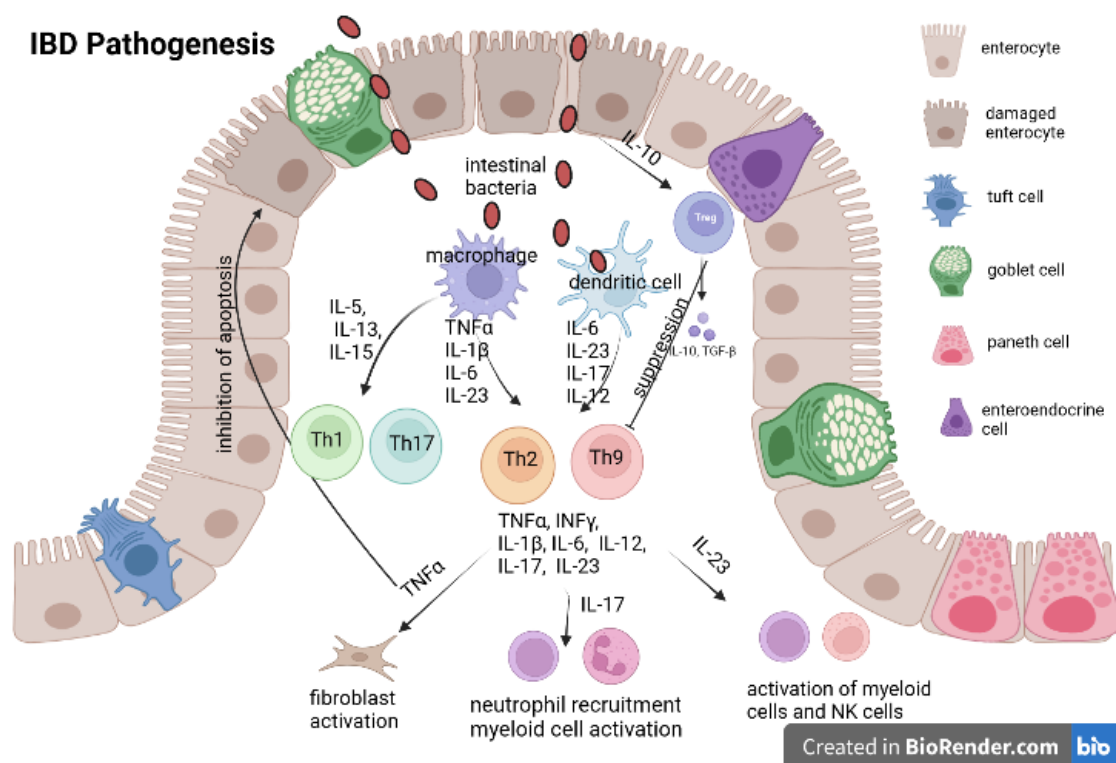


Figure 3- IBD Pathogenesis. The inflammation pathway in IBD is complex. Specific intraluminal pathogens are believed to interact with immune cells and trigger the inflammatory process. A complex network of cells and cytokines is involved. Crohn's disease is a Th1-driven immune response, whereas Ulcerative Colitis is a Th2-driven response.

1.3 Clinical Features of IBD

As the introduction mentions, IBD is a chronic inflammatory disease of the Gastrointestinal System. The first described IBD type, Ulcerative Colitis, involves continuous inflammation

that affects the mucosa of the large intestine and rectum.⁴⁸ The other major IBD type, Crohn's disease, is characterized by inflammation of the lining of the digestive tract, at any segment of the GI tract, from the mouth to the anus. The inflammation can be deeper than the mucosal level and affect all four layers of the digestive tract.⁴⁹

IBD symptoms vary, depending on the location and the severity of inflammation. In addition, in the clinical course of the disease, IBD patients often experience periods of active disease followed by periods of remission.

Symptoms and signs common in both UC and CD include persistent diarrhea, blood in the stool, abdominal pain or cramping, as well as systemic symptoms such as fatigue, reduced appetite, and unintended weight loss.^{48,49} Except for these symptoms, many patients also experience one or more extra-intestinal manifestations (EIMs), including the dermatological system (erythema nodosum, pyoderma gangrenosum), the ophthalmological system (uveitis, scleritis), the hepatic system (sclerosing cholangitis), and the musculoskeletal system (spondylarthritis, peripheral arthritis).⁵⁰ Although the EIMs are frequent, prevalence has not been extensively studied. According to Bernstein et al., 6 to 40% of IBD patients have at least one extra-intestinal manifestation.⁵¹

If IBD is left untreated, patients experience the progression of inflammation, irreversible bowel damage, and long-term complications. Persistent symptoms from both the GI tract and the extra-intestinal systems significantly impact patient Quality of Life (QoL) and patient survival. Abdominal pain is a common persistent gastrointestinal symptom. Regardless of disease severity, up to 60% of IBD patients report daily abdominal pain, which affects their QoL.⁵² Other Long-term complications from the digestive system that patients may suffer from include the presence of an abscess (perianal or intrabdominal), the presence of a fistula (perianal or fistula that connects the bowel with the skin or any other intrabdominal system), the presence of bowel stricture or bowel perforation. These complications are associated with

a high risk of surgery. Long-term complications that affect the extra-intestinal systems include chronic, difficult-to-treat skin lesions, chronic eye issues, hepatic disease (such as liver cirrhosis and cholangiocarcinoma), and chronic painful musculoskeletal issues such as osteoporosis and permanent joint deformities. In addition, there are some systematic long-term complications, such as malnutrition and malabsorption, anemia, and psychological imbalance. Furthermore, it is reported that the risk of colorectal malignancy is unacceptably high in IBD patients who do not control their bowel inflammation.⁵³⁻⁵⁵ Finally, IBD patients can develop extra-intestinal cancer, regarding individual cancer types, and some factors, including extra-intestinal manifestations, can explain this.^{55,56}

1.4 Treatment in IBD

1.4.1 “Treat-to-target” strategy

Since IBD is not a curable disease, the goals of treatment of Crohn’s disease and Ulcerative Colitis are to control the inflammation and achieve clinical remission, endoscopic/biochemical remission, and ideally histologic remission. In the best cases, this may lead to symptom relief and improvement of QoL, but also to long-term remission and reduced risk of complications. Clinical remission is the absence of symptoms and normalization of the primarily symptom-based disease activity indices, such as the CD activity index (CDAI) and the Simple Clinical Colitis Activity Index (SCCAI). Endoscopic remission or “mucosal healing” is characterized by the absence of signs of intestinal inflammation assessed by examination, like a colonoscopy. Evidence of intestinal inflammation is mucosal erythema, mucosal edema, and the presence of ulcerations. There are also endoscopy-based disease activity indices, such as the Simple Endoscopic Severity Index for CD (SES-CD) and the Mayo Endoscopic score for UC. According to a recent study, mucosal healing was associated with a lower risk of new

bowel stricture or perforation and thus lower frequency of surgery.⁵⁷ The review of Carvalho et al. exacerbated the benefit of mucosal healing, as mucosal healing leads to a lower frequency of flares, hospitalization, and surgery.⁵⁸ The significance of histologic remission, though, is controversial. It is suggested that histological remission can assess the risk of disease-related complications and outcomes.⁵⁹ However, studies have shown that microscopic inflammation persists in various cases of endoscopically quiescent disease.⁵⁹⁻⁶¹ Consequently, a “treat-to-target” strategy is to achieve “steroid-free” clinical, endoscopic remission and ideally, histologic remission because this is associated with improved QoL and better outcomes.⁶²

1.4.2 Therapeutic options

1.4.2.a Aminosalicylates

Aminosalicylates include sulfasalazine and 5-Aminosalicylic Acids (5-ASA) drugs. This medication has been used as IBD treatment for 80 years,⁶³ to treat mild-to-moderate colitis. The mechanism of action includes inhibition in the metabolism of arachidonic acid, inhibition of cytokine production, and scavenging of reactive oxygen species.⁶⁴ In addition, a recent experimental study showed that mesalamine can induce regulatory T cells in the colon and activate the anti-inflammatory TGF- β cytokine.⁶⁵

IBD patients treated with 5-ASA may experience mild side effects, such as flatulence, nausea, abdominal pain, diarrhea, and headache.⁶³ A more severe side effect is developing nephrotoxicity within one year of mesalamine treatment.⁶⁶ Patients treated with sulfasalazine may develop hemolytic anemia, photosensitization, and temporary infertility.⁶³

1.4.2.b Corticosteroids

Corticosteroids have been used as a therapeutic option for IBD since the 1950s.⁶³ Their mechanism of action is based on the activation of the corticosteroid receptors of the

cytoplasm, which enter the nucleus and inhibit the transcription of inflammatory genes, regulating the activation of lymphocytes and the expression of inflammatory cytokines.^{63,67}

Oral corticosteroids are used as a short-term treatment for IBD because they can induce remission quickly, but they are not recommended for long-term treatment due to their lack of effect in maintaining remission and their side effects.^{63,68,69}

Corticosteroid side effects are numerous and include weight gain, facial edema (“moonfaced”), thin and dry skin, as well as hypertension, hyperglycemia and diabetes mellitus, opportunistic infections, osteoporosis, venous thromboembolism and many others.⁷⁰

1.4.2.c Immunomodulators

Immunomodulators, also called immunosuppressants, are types of IBD medication that can modify the activity of the immune system. They can interfere with DNA synthesis and inhibit lymphocyte proliferation, decreasing the inflammatory response.⁶³ Thiopurines (azathioprine and 6-Mercaptopurine) were the first immunomodulators used widely in IBD. They are effective therapeutic options for maintaining remission in IBD but aren’t used for inducing remission due to their slow onset of action.⁷¹ Concerning their side effects, thiopurines can cause bone marrow suppression, liver injury, pancreatitis, and gastrointestinal intolerance.⁷² Other immunomodulators to treat IBD are Methotrexate and calcineurin inhibitors (cyclosporine A and tacrolimus). Methotrexate can inhibit several enzymes related to DNA synthesis,⁶³ whereas calcineurin inhibitors prevent the calcineurin-activated enzyme from regulating the transcription of inflammatory genes. As a result, they downregulate various inflammatory cytokines, inhibiting lymphocyte activation and inflammatory response.⁷³ Among the reported side effects, the possibility of renal function damage, hyperkalemia, and some infectious diseases, make close monitoring of immunosuppressant-treated IBD patients inevitable.⁷³

1.4.2.d Biologic Anti-TNF Therapy

As mentioned above, Tumor Necrosis Factor (TNF) is a key proinflammatory cytokine that plays an important role in the inflammation process in several diseases, including IBD.⁶³ Anti-TNF therapeutics, Infliximab and Adalimumab, were the first anti-TNFs used in IBD. They are monoclonal antibody therapies that block TNF. However, the mode of their action is likely to be more than just the binding of TNF. They also induce apoptosis of cells expressing membrane TNF.⁷⁴ Apart from common adverse events such as headaches, nausea, diarrhea, and abdominal pain, anti-TNFs are associated as well with serious adverse effects, including serious infections, congestive heart failure, drug-induced lupus (with the characteristic butterfly-shaped rash on cheeks and nose), other skin reactions, demyelinated disorders, and malignancies.⁷⁵

Although anti-TNFs are considered an effective therapeutic option, some patients never respond to this therapy, and unfortunately, it is not known in advance. According to a recent study investigating the mechanisms responsible for anti-TNF therapy failure, up to 40% of patients in clinical trials and 10-20% of patients in clinical series don't respond to this biologic therapy from the beginning.⁷⁶ Another issue is the Loss-of-Response (LOR) in about 23-46% of IBD patients in the first year,⁷⁶ which requires some therapeutic management and changes like dose increase and shortened dose interval.

1.4.2.e Biologic Anti-IL-12/23 Therapy

IL-12 and IL-23 cytokines play a major role in IBD due to their pro-inflammatory action, which induces intestinal inflammation. Thus, the anti-IL-12/23 biologic agents have been proven very effective.

Ustekinumab is a fully humanized IgG monoclonal antibody, approved for moderate-to-severe IBD, which binds to the common 40 subunit of IL-12 and IL-23, preventing the connection with their receptor located on the membrane of T cells and NK cells. As a result, the activation and infiltration of these immune cells is inhibited.⁷⁷ Real-world studies showed that Ustekinumab is safe and effective because 34% of CD and 39% of UC patients achieved clinical remission after Ustekinumab induction, with a few reported severe adverse effects.⁷⁸ Nevertheless, there is still a significant percentage of IBD patients who were exposed to this substance, and they didn't respond.

A new recently approved- monoclonal antibody therapy for IBD is Risankizumab which is a selective IL-23 inhibitor already used by dermatologists for treating psoriasis.⁷⁷ There are many clinical trials, including psoriatic patients treated with Risankizumab. The study results showed both short-term and long-term benefits related to inflammation without negative interactions for the GI system.⁷⁹ Furthermore, early clinical trials support the efficacy of Risankizumab on induction and maintenance of remission in IBD.⁸⁰ Interestingly, a study from the USA found in 2022 that IBD patients who are anti-TNF inadequate responders achieve remission after treatment with Risankizumab.⁸¹ Considering this fact, it would be beneficial to know in advance which IBD patients will benefit from anti-TNFs and which ones will benefit from IL-23 inhibitors.

1.4.2.f Biologic Anti-integrin therapy

Integrin is a cell surface glycoprotein expressed by T lymphocytes, which helps T cells enter, and the T cells enter and trafficking to the intestinal mucosa. Specifically, the $\alpha 4\beta 7$ integrin binds to Mucosal addressing Cell Adhesion Molecule 1 (MadCAM-1), mediating the infiltration of leukocytes onto the intestinal mucosa.^{82,83} Vedolizumab, a recombinant human IgG1

monoclonal antibody, reduces lymphocyte infiltration and intestinal inflammation by binding to the $\alpha 4\beta 7$ integrin and inhibiting its interaction with MadCAM-1.^{82,83} Vedolizumab is considered safe and effective in treating IBD and a recent study showed that patients who failed TNF-inhibitors therapy, achieved remission by using anti-integrin therapy.⁸⁴ However, disadvantages like primary no-response, secondary LOR, and drug intolerance require further research to generate novel therapeutic options.⁶³

1.4.2.g Small molecules- JAK inhibitors

The JAK-STAT signaling pathway involves Janus Kinase (JAKs), Signal Transducers and Activators of Transcription (STATs) proteins and receptors. Initially, cytokines, like interferon and interleukins, activate JAK receptors, and the recruitment of JAK kinases activates STATs proteins leading to the translocation of these proteins to the cell nucleus and transcription of inflammation genes.⁸⁵ There are four members in the JAK family (JAK1-3 and tyrosine kinase 2) and seven members of the STAT family (STAT 1-4, STAT5 A/B, STAT6). JAK inhibitors are novel therapeutic options that target the JAK family kinases interfering with the JAK-STAT signaling pathway.

Tofacitinib was the first JAK inhibitor used and inhibits all JAKs, preferentially JAK1 and JAK3, and it was approved in 2018 for treating moderate to severe Ulcerative Colitis.⁸⁵ According to a systematic overview of meta-analyses in 2019, tofacitinib was superior to placebo in controlling intestinal inflammation and leading to mucosal healing.⁸⁶ However, there is a concern about tofacitinib adverse effects, including herpes zoster and thrombosis (deep vein thrombosis or pulmonary embolism).⁸⁷

Upadacitinib is a new promising selective JAK-1 inhibitor, which has recently been approved for moderate-to-severe Ulcerative Colitis. Data from a randomized trial of 250 patients with UC showed the efficacy of Upadacitinib with endoscopic improvement at week 8 compared to

placebo. Furthermore, similarly to Ustekinumab, Wang et al. study found that Upadacitinib could affect upregulated mechanisms in IBD patients who respond inadequately to anti-TNFs.⁸¹ Concerning side effects, one event of herpes zoster and one event of thrombosis were reported in the clinical trial of Sandborn et al. In addition, increased serum lipid levels and creatinine phosphokinase levels were observed.⁸⁸

1.4.2.h Surgical Management

The significant progress in medical treatment of IBD led to lower rates of surgical management of the disease. According to an 8-year study, the percentage of CD patients who underwent a surgical approach for their disease decreased from 10 to 8.8%, whereas the relevant portion of UC patients dropped from 7.7 to 7.5%.⁸⁹ Nevertheless, surgery is still an important and sometimes the best therapeutic option. Regarding Ulcerative colitis, the absolute indications for surgery include massive intestinal bleeding, bowel perforation, proven colorectal cancer, or highly suspected colonic malignancy. Relative indications are severe disease or toxic megacolon non-responding to medical treatment and poor outcomes or serious adverse events from the medical approach.⁹⁰ Regarding Crohn's disease, the most common intestinal resection is the ileocecal resection with primary anastomosis. The indication is failed medical treatment, disease relapse after medical treatment, or patient preference.⁹⁰

1.4.3. Novel therapies

Since no curative treatment for IBD exists, research efforts are directed to multiple alternative therapies. In a few words, novel therapies target the abstraction of the inflammatory factors, the alteration of the trigger factors, or the transplantation of the affected cells.

A first example is apheresis therapy, which targets removing the specific leukocytes involved in the inflammatory process from the patient blood circulation.⁹¹ Another alternative treatment is using antibiotics, probiotics, or even Fecal Microbiota Transplantation (FMT) to change the intestinal microenvironment.⁶³ FMT targets to replace the IBD patient microbiome with the intestinal ecosystem of healthy individuals. Stem Cell Transplantation is another novel therapeutic technique that can replace inflamed IBD tissue and restore the normal physiology process. Mesenchymal Stem Cells derived from bone marrow, umbilical cord, or adipose tissue can be directed to specific tissue and act as 1) cell providers for restoring the integrity of the damaged tissue, 2) immune moderators by regulating the immune response in the target tissue, and 3) trophic resource.⁹² Intestinal Stem Cells (ISCs) can also be transplanted and replace the inflamed IBD epithelium because they can differentiate into all cell types of the intestinal epithelium. When Sato et al. used the ISCs derived from biopsy tissue during a colonoscopy, they developed a 3D structure and studied the intestinal microenvironment *in vitro*, which was similar to the *in vivo* microenvironment.⁹³ So, Yui et al. study used murine ISCs and transplanted them to the recipient intestinal epithelium, showing that the graft was functionally and histologically normal.⁹⁴

Although the above results are impressive, they are still in research progress and can't be applied to the clinical management of patients. Currently, disease management is based on existing medications, but new therapeutic options are emerging. However, not all patients respond to this medical approach indicating the need for improved therapies and personalized therapy. There are a few animal models for further study of IBD and testing of IBD medication. However, animal models do not recapitulate human disease and do not respond to medication exactly like the human body. As a result, there is a need for newer and more clinically relevant models which can incorporate human disease tissues. These

alternative research models can be used for mechanistic studies and screening new therapeutics before their application in clinical practice.

1.5. Research tools for personalized medicine

The existing research tools for personalized medicine are the *in vivo* Animal Models, the *in vitro* 2D-Models, and the 3D-Models (Figure 4). These experimental models try to mimic the human intestinal epithelium. The intestinal epithelium consists of a single layer of cells that form the crypt-villus structure, which can absorb the diet nutrients. The crypt-villous structure is quickly renewed every 4-5 days and consists of terminally differentiated functional cell types, including enterocytes, enteroendocrine cells, goblet cells, tuft cells, and other cell types. (Figure 3) The Intestinal Stem Cells located at the bottom of the crypt move up toward the tip of the villus while differentiating. Finally, when they reach the villus's tip, they mature and die, shedding off into the intestinal lumen. Although there are no villous structures in the large intestine, the architecture of the epithelium is similar to the small intestine, with the ISCs at the bottom of the crypts.

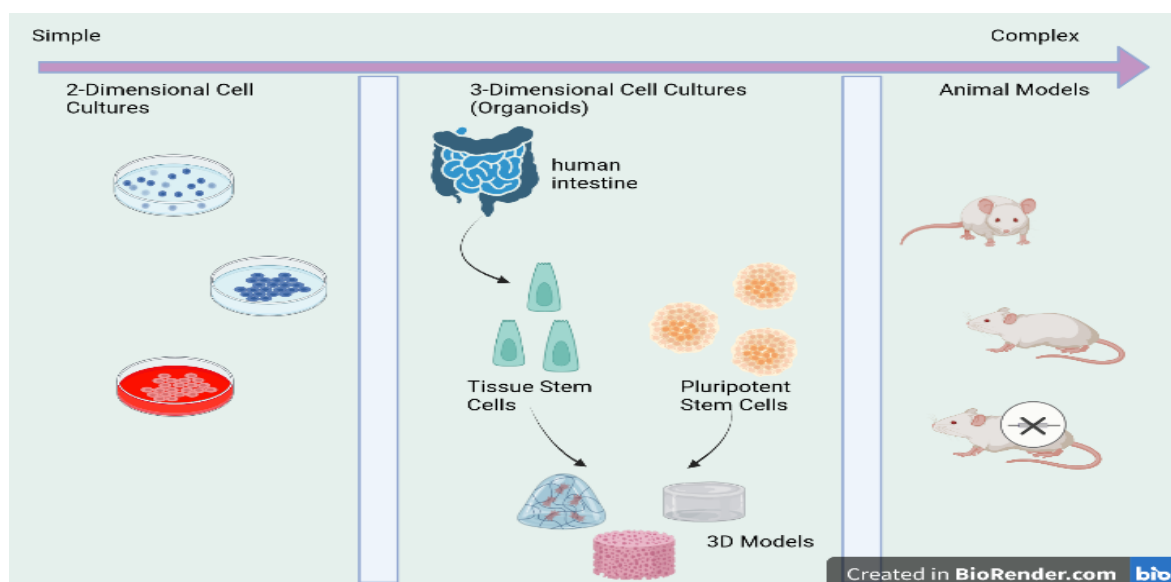


Figure 4-Research tools include 2-Dimensional culture Systems, 3-Dimensional Culture Systems, and Animal Models.

1.5.1. Animal models

Animal models are a helpful tool used in translational research studies in general and, more specifically, gastrointestinal studies.⁹⁵ For example, a cancer development study *in vivo* can be done using xenografts, in which human cancer cells are transplanted to immunosuppressed mice models.⁹⁶ Regarding IBD, the animal experimental models contribute to the study of the disease and develop and screen novel therapeutics. Rabbits were the first animal experimental model for inducing colitis in 1957. However, the most used experimental model is with genetically modified mice, which develop spontaneous colitis and/or ileitis.⁹⁷ In a few words, there are different experimental models. There are chemically induced experimental models where inflammation is induced after using specific substances that trigger immune response. The administration of particular substances results in the induction of a highly reproducible acute inflammation localized in the colon. The inflammation is induced shortly after the substance administration. However, there are some limitations, such as closely monitoring the batch of chemicals and other parameters. There are also the Immunological Models, where specific CD4⁺ T-cells are transferred from donor mice to lymphopenic mice recipients. The model limitation has to do with the fact that the immunodeficient recipients can't simulate the whole pathogenesis of colitis. Genetically Engineered Experimental Models are frequently used in experimental animal models, including the "knockout models". In this case, the development of murine models deficient in a specific gene allows the study of the relevant pathogenesis pathway. However, one limitation of this model is the long time needed for the development of this model. In addition, we should consider the variability in the development of colitis between humans and mice. In humans, colitis is associated with multiple gene involvement. In contrast, studies in mice use models deficient in only a specific gene. Finally, there are the Microbiome-induced models, where the intestinal microbiota of the animal models is changed.⁹⁷ This model provides the

opportunity to study the link between microbiota and intestinal inflammation, but the way the murine intestine reacts is different compared to the human one. Other limitations concerning the use of murine models are the fact that there is a large discrepancy between human and animal immune responses and also the fact that there are multiple environmental factors in humans, such as drugs and smoking, that cannot be precisely reproduced in mouse models.⁹⁷

In conclusion, animal models cannot be regarded as good models for studying IBD because they cannot completely simulate the disease.

1.5.2. 2D Models

2-Dimensional (2D) cell cultures have been used since the early 20th century and allow observing how cells communicate and interact. The technique requires breaking down the original tissue to extract the cells and let them in a simplified environment without surrounding cells and their products.⁹⁸ These cells come from a primary cell culture because they are directly isolated from the original tissue. However, cell culture can originate from a cell line, meaning that the total of cells originates from a single common ancestor cell. The studied cells are cultured in a dish and proliferate as a monolayer in two dimensions. However, 2D culture systems don't allow long-term culture. Cells must modify their complex biological functions (i.e., apoptosis) and require exogenous nutrients and growth factors to expand *in vitro*.⁹⁹

Researchers have tried establishing 2D monolayer culture systems with improved features to overcome these limitations.¹⁰⁰ The standard method is to culture cells on an extracellular matrix-coated surface.¹⁰⁰ Based on this technique, Scott et al. developed an intestinal epithelial monolayer on a plate coated with Collagen I.¹⁰¹ Another technique using Collagen I

as a matrix is the transwell system that allows independent access to both sides of a cell monolayer.¹⁰² In addition, Liu et al. developed the 2D intestinal epithelium on a thin layer of Matrigel, which is the solubilized basement membrane matrix secreted by Engelbreth-Holm-Swarm (EHS) mouse sarcoma cells.¹⁰⁰ Finally, Wang et al., using the transwell-based 2D Model, developed a columnar epithelium with villous-like structures.¹⁰³ The model advantages are that the villous-like structures can simulate the human epithelium and that the monolayer surface allows cell exposure to pathogens as well as the administered medication.¹⁰⁰ However, a limitation to be considered is that the monolayer cell structure doesn't mimic the natural tissue structure, and the cultured cells alter their morphology, and their interaction with other cells and the extracellular environment.¹⁰⁴

1.5.3. 3D Models

Between Animal Models and 2D models are the 3-Dimensional- based culture Systems. The 3D Models can mimic the natural tissue and serve as a tool for studying the physiological properties and conditions, facilitating either developmental or disease progression processes. They can also be used as a screening platform for new medications before their application to animal studies or clinical practice.⁹⁹ The first 3D culture system was presented in 1992 by Petersen and Bissel, and it was a system for studying normal and malignant human breast tissue.¹⁰⁵

In general, there are two major 3D culture systems: the scaffold-free and the scaffold-based cultures, depending on the technique they are formed.¹⁰⁶ Scaffolds in engineered tissues resemble natural Extracellular Matrix (ECM) and can support the 3D Model architecture and provide mechanical and shape stability to the cultured cells.¹⁰⁷ Furthermore, scaffolds consist of biomaterials compatible with cell components, and as a result, they facilitate and regulate

cellular activities.¹⁰⁷ The biomaterials used are hydrogels, which are polymer networks that allow cells to be embedded. These polymer networks are not cross-linked, and as a result, they enable soluble factors such as cytokines and growth factors to pass through the material.¹⁰⁸ In addition, due to this hydrophilic permeability, hydrogels swell widely, forming stable 3D structures.¹⁰⁹ Hydrogels can be classified into different categories, which are the ECM protein-based hydrogels (including laminin and collagen), the natural Hydrogels (including Matrigel, gelatin, alginate, etc.), and the synthetic Hydrogels.⁹⁹

3D Models can also be divided into Patient-Derived Xenografts (PDX) 3D Models, Spheroids 3D Culture Models, and Organoids 3D Culture Models based on the cell origin and the cell structure inside the model.¹⁰⁰ The PDX 3D models consist of the patient's cells (mostly tumor cells) implanted in immunodeficient hosts (usually mice).¹⁰⁰ They are characterized by *in-vivo*-like complexity, and their advantages are that they recapitulate human disease and tumor heterogeneity, and model response results are similar to patient response.¹¹⁰ Spheroids 3D Culture Models consist of cells from tumor cell lines or tumor biopsies that are self-assembled in aggregates freely floating in ultra-low attachment plates. Spheroids 3D Models may or may not contain extracellular matrix.¹¹⁰ On the other hand, organoids are more complex and more *in vivo*-like structures. They are formed by pluripotent stem cells, tumor cells, or tissues, and they are self-assembled, self-organized, and differentiated in response to physical and chemical factors. The organoid 3D Culture models require ECM (i.e., Matrigel) and signaling pathways, including proteins and growth factors.¹¹⁰ Organoid 3D Models rely on the ECM to keep the tissue microenvironment's geometric, mechanical, and biochemical conditions.

1.5.4. Comparison of the existing research tools

The improvement in personalized medicine research led to the optimization of the previous research tools and the generation of new ones, but each research tool type has strengths and weaknesses. Based on the goal of IBD personalized medicine, 3D Culture Models have become superior compared to *in vivo* animal models and *in vitro* 2D models by providing more physiological and clinically relevant data while also reducing the number of animals used in follow on preclinical work.

Compared to *in vivo* animal models, 3D Culture Systems, especially organoids, are more applicable to the intestinal epithelium. Although mouse intestinal epithelium shares many biological and histologic traits with human intestinal epithelium, there are crucial differences in mechanisms associated with the renewal of human intestinal stem cells.⁹⁵ Furthermore, organoid 3D Models serve as a platform for observing the development of crypt morphogenesis on the microscope. Finally, a significant advantage of 3D Culture Systems is that they serve as high-throughput screening platforms for novel therapeutics. Organoids can be plated in large multiplex arrays in contrast to the massive use of mouse models that raises issues such as animal ethics, interventional procedures, and high cost.⁹⁵

Compared to 2D Model cells, cells cultured in 3-Dimension Systems are well-differentiated, and their proliferation rates resemble those of the human body. 3D Models allow not only intracellular interaction study but also cell-matrix interaction study.¹¹¹ Using 3D co-culture models, the interaction between different cell types is also feasible. In addition, 3D Culture Systems imitate the natural tissue microenvironment; thus, drug distribution and heterogenous cell exposure resemble real conditions.⁹⁹ Limitations of using the 3D Culture Systems are less ability to manipulate the experiment models and higher cost of generating these models.¹¹²

CHAPTER 2

METHODS

2.1 Objective of the Study and clinical significance

IBD therapy has improved in the last few years but still has significant limitations. The variety in therapeutic options means that the perfect IBD treatment hasn't been found, and many patients don't respond to the initial therapies or lose response during the treatment. In other words, many patients must try different IBD therapies to achieve remission. They may experience the side effects of the inappropriate medication or face complications of the disease progression due to inadequate treatment response. Consequently, there is an urgent need to generate a screening platform for therapeutics before their use in clinical practice.

Due to the lower proliferation rate of IBD patient-derived cells, colorectal adenocarcinoma cells could be used instead of IBD cells, at least initially. Colorectal adenocarcinoma cells have a higher proliferation rate, and they can be used for generating and testing a 3D Model before its application to IBD. The fundamental hypothesis is that a 3D co-culture of gut epithelial and stromal cells will produce a bio-mimetic physiological gut model responsive to inflammation and anti-inflammatory therapeutics. To prove our hypothesis, the first thing to be done is to determine bioink compatibility for isolated human cancer intestinal epithelial cells and basement membrane fibroblast cells. Therefore, we tested alginate and gelatin bioinks for cell viability, metabolic activity, and cell proliferation. Our second objective was to determine 3D culture model compatibility for mimicking the gut microenvironment. For that reason, we measured the expression of cytokines to assess the model response to inflammatory factors, followed by the use of anti-inflammatory therapies.

2.2 Objective 1- Generation of 3D culture models

2.2.1 Materials that were used

2.2.1.a HT-29 cell line

The HT-29 cell line is a human adenocarcinoma cell line first isolated by Fogh and Trempe in 1964 from a 44-year-old female's primary tumor.¹¹³ This cell line has been used in research because of its ability to grow easily in laboratory conditions, differentiate and thus simulate real colon tissues *in vitro*.^{114,115} These cells can grow and form a multilayer of nonpolarized cells with an undifferentiated phenotype on an electronic microscope. However, after stimulation with specific growth factors, they express distinct pathways of enterocyte differentiation.¹¹⁶ Interestingly, the HT-29 cell line has been proven to promote fibroblast proliferation due to the expression of fibroblast stimulating factors. Thus a co-culture of the HT-29 cell line with fibroblasts is interesting to be studied.^{117,118} Concerning cytokine production, it has been shown that HT-29 cells secrete pro-inflammatory cytokines, such as TNF α and IL-6, and these cytokines can further promote tumorigenesis. Other cytokines, such as IFN- γ and IL-12, have antitumorigenic properties.^{37,113} However, the contribution of other cytokines, such as IL-1, to CRC development and progression is not yet known.³⁷

Our study cultured the HT-29 cell line in a 2-Dimensional Culture System before using it in our 3D models (Figure 5). As growth medium (culture medium), we used Dulbecco's modified Eagle's medium containing 4.5 g glucose/liter and supplemented with 10% Fetal Calf Serum (FBS) and penicillin/streptomycin (100 units/mL of penicillin and 100 μ g/mL of streptomycin).¹¹⁸ Initially, we used a vial of 1,000,000 HT-29 cells frozen with a 10% Dimethyl Sulfoxide (DMSO) Solution. The vial, stored in liquid nitrogen, was thawed in a 37 °C water bath. Afterward, the vial content was aspirated and mixed with fresh culture medium, and the cells were centrifuged at 500 x g for 5 min. After centrifugation, we removed the supernatant

medium and diluted the cell residue with 1ml growth medium mixing well with a pipette. We seeded the cell suspension in a T-75 flask and cultured the cells at 37 °C in a humidified cell culture incubator with 5% CO₂. We changed the growth medium every 2-3 days.

Passaging was performed when the HT-29 cells reached 80% confluency. First, we removed the existing culture medium, washed the cells with sterile PBS, and detached them using 0.25% trypsin (Gibco, Burlington, ON, Canada). After a 3-minute incubation in trypsin solution at 37 °C in a humidified cell culture incubator with 5% CO₂, we collected the cell suspension and centrifuged at 500 x g for 5 min. After centrifugation, we removed the supernatant medium and diluted the cell residue with a 2ml growth medium mixing well with a pipette. We aspirated 15µl of the suspension and mixed it with 15µl Trypan Blue (ThermoFisher, ON, Canada). Then we applied the 30 µl solution to a hemocytometer's edge and determined the number of cells per chamber by direct counting using a microscope. We calculated the concentration of cells in the original mixture using the formula:

The concentration of cells in the original mixture = [(number of cells counted x dilution factor) / number of chambers] x 10,000.

After calculating the total number of cells in the original mixture, we aspirated 400,000 cells to seed in our 2D culture. We seeded 400,000 HT-29 cells in a T-75 flask, added 10ml culture medium, and cultured the cells at 37 °C in a humidified cell culture incubator with 5% CO₂ until we set the experiment of generating the 3D culture model.

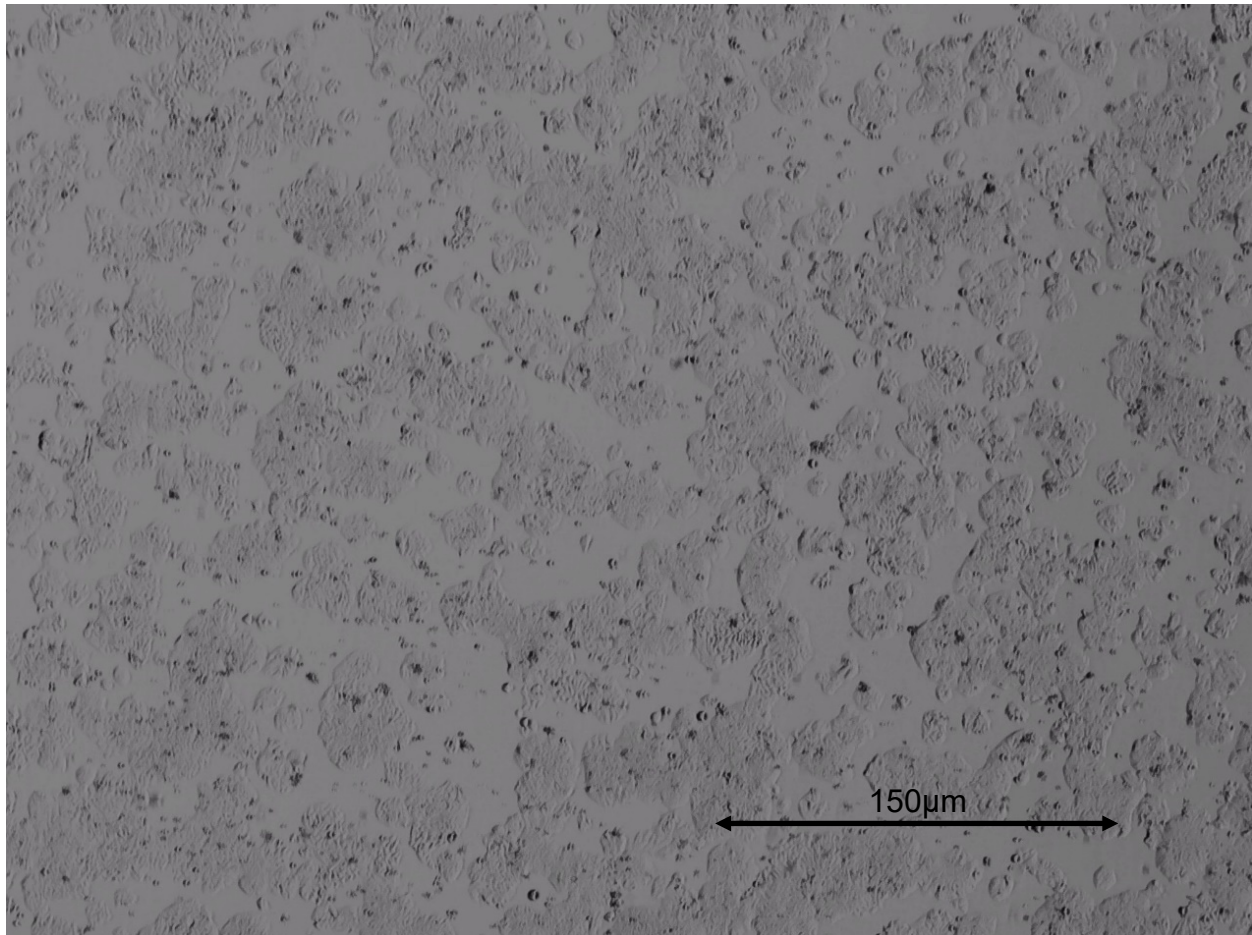


Figure 5: HT-29 cell line – 2D culture

2.2.1.b IRM-90 cell line

The IRM-90 cell line is a human fibroblast cell line derived from the normal lung tissue of a 16-week-old female. Fibroblasts come from primitive mesenchyme, the predominant stromal cell type in soft connective tissues.¹¹⁹ On microscope, active fibroblasts form plump spindle- or stellate-shaped cells with centrally placed oval or round nuclei. However, their morphology and function might differ depending on the *in vivo* location.¹¹⁹ In general, fibroblasts secrete extracellular matrix precursors, contributing to connective tissue's structural integrity. More specifically, fibroblasts produce the components of ECM, namely the structural proteins, adhesive proteins, and a space-filling ground substance consisting of proteoglycans and glycosaminoglycans.¹²⁰ Structural proteins (e.g., fibrous collagen and elastin) form a network of protein fibers and connector proteins that provide structure

to the tissue. Fibroblasts may produce different quantities of collagen subtypes and elastin based on the rigidity of each tissue.¹²¹ Interestingly, in inflammatory conditions, there is a disbalance in structural protein production followed by fibrosis.¹²¹ Adhesive proteins, such as fibronectin and laminin, mediate the connection between cells and the ECM. Fibronectin also regulates Tumor Growth Factor- β (TGF- β) expression and collagen assembly. Laminin holds cell attachment to the basal lamina.¹²⁰ Fibroblasts also produce the ground substance of ECM, which consists of a hydrated gel of proteoglycans connected with unbranched polysaccharides called glycosaminoglycans. The space-filling ground substance is mixed with the structural proteins, allowing intracellular communication and nutrient flow from blood circulation into the tissue.¹²⁰

Our study used the IRM-90 mCherry fibroblasts because of their unique feature. mCherry belongs to a Red Fluorescent Proteins (RFP) family derived from *Discosoma* sp. coral (DsRed).¹²² The RFPs were discovered in 1999, but the mCherry protein is the most widely used one. It is constitutively fluorescent, visualized red-orange when excited, and is photostable, conferring good quality on a microscope for long-term studies.¹²² It is also a versatile biological marker that facilitates monitoring physiological processes and identifying protein localization on a fluorescent microscope.¹²³

Our study cultured the IRM-90 cell line in a 2-Dimensional Culture System before using it in our 3D models (Figure 6). As growth medium (culture medium), we used Dulbecco's modified Eagle's medium containing 4.5 g glucose/liter and supplemented with 10% Fetal Calf Serum (FBS) and penicillin/streptomycin (100 units/mL of penicillin and 100 μ g/mL of streptomycin).¹¹⁸ Initially, we used a vial of 1,000,000 IRM-90 fibroblast cells frozen with 10% Dimethyl Sulfoxide (DMSO) Solution. The vial, stored in liquid nitrogen, was thawed in a 37 °C water bath. Afterward, the vial content was aspirated and mixed with fresh culture medium, and the cells were centrifuged at 500 x g for 5 min. After centrifugation, we removed

the supernatant medium and diluted the cell residue with 1ml growth medium mixing well with a pipette. We seeded the cell suspension in a T-75 flask and cultured the fibroblasts at 37 °C in a humidified cell culture incubator with 5% CO₂. We changed the growth medium every 2-3 days.

Passaging was performed when the IRM-90 fibroblast cells reached 80% confluency. First, we removed the existing culture medium, washed the cells with sterile PBS, and detached them using 0.25% trypsin (Gibco, Burlington, ON, Canada). After a 3-minute incubation in trypsin solution at 37 °C in a humidified cell culture incubator with 5% CO₂, we collected the cell suspension and centrifuged at 500 x g for 5 min. After centrifugation, we removed the supernatant medium and diluted the cell residue with a 2ml growth medium mixing well with a pipette. We aspirated 15µl of the cell suspension and mixed it with 15µl Trypan Blue (ThermoFisher, ON, Canada). Then we applied the 30 µl solution to the edge of a hemocytometer and determined the number of fibroblasts per chamber by direct counting using a microscope. We calculated the concentration of cells in the original mixture using the formula:

Concentration of cells in the original mixture = [(number of cells counted x dilution factor) / number of chambers] x 10,000.

After calculating the total number of cells in the original mixture, we aspirated 300,000 fibroblast cells to seed in our 2D culture. We seeded 300,000 IRM-90 cells in a T-75 flask, added 10ml culture medium, and cultured the cells at 37 °C in a humidified cell culture incubator with 5% CO₂ until we set the experiment of generating the 3D culture model.

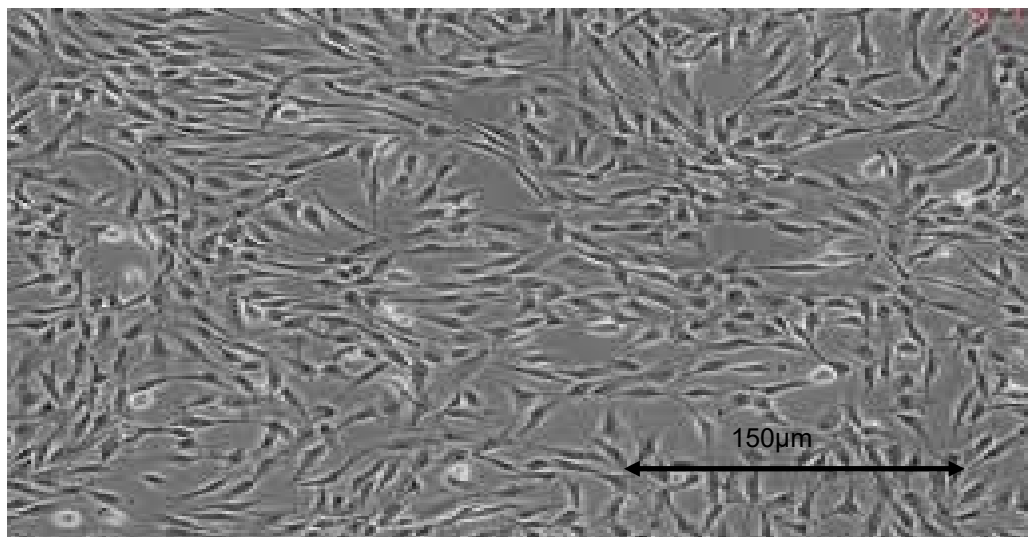


Figure 6: mCherry IRM-90 Fibroblast cell line-2Dculture

2.2.1.c Alginate-Gelatin Hydrogel

Hydrogels are excellent materials for 3D *in vitro* cell cultures. As mentioned above, they can absorb water and nutrient-containing fluids. As a result, they support cell proliferation and mimic the natural microenvironment of tissue ECM.⁹⁹ Among the different materials used in hydrogel manufacture, we chose the combination of alginate (polysaccharide) and gelatin (polypeptide).

Alginate is a polysaccharide found in seaweed or bacteria.¹²⁴ Alginate is used because it can retain water and is biocompatible, biodegradable, and non-toxic. However, alginate hydrogel has poor long-term stability in physiological conditions due to its biodegradability.¹²⁵ Furthermore, the low adhesive ability could limit alginate application. Hydrogel's physical and mechanical properties can be improved by combining alginate with other materials.¹²⁴ Gelatin is such a biomaterial. Gelatin is a polypeptide produced after hydrolysis of animal collagen due to its collagen origin, and it facilitates cell adhesion, proliferation, and differentiation. It is also biocompatible, biodegradable, and non-toxic, and it remains in a gel state condition at a temperature below 40 °C.¹²⁴ The use of a cross-linking agent is crucial due to the fast degradation ability of gelatin. Combining alginate and gelatin can enhance hydrogel's benefits and overcome each biomaterial's deficits. For

example, combining gelatin with alginate will improve insufficient cell attachment. Also, alginate-gelatin hydrogel stiffness promotes cell differentiation to specific lineages¹²⁶ and facilitates cell-to-cell interaction as well as the interaction between cell and ECM. Subsequently, drugs and metabolism components (e.g., oxygen, wastes) can be diffused. Furthermore, co-culture generation leads to multiple-cell interaction, mimicking the tissue microenvironment.¹²⁴ According to Jiang et al., the composition of the bioink was set to 1 w/v% of alginate and 7 w/v% of gelatin (A1G7) because they promote a high cell proliferation rate and prolonged cell survival.¹²⁷ In our study, we used 50ml PBS warmed at 80 °C and added 0.5 g alginate under continuous stirring. When alginate was completely dissolved (approximately 1 hour later), we decreased the solution temperature to 40 °C and added 3.75 g gelatin under constant stirring. When gelatin was completely dissolved, the A1G7 Hydrogel was sterilized under Ultraviolet (UV) Light for 24 hours. The Hydrogel was stored at 4 °C.

2.2.1.d Cross-linking agent and culture medium

However, as mentioned above, the generation of the hydrogel model needs a cross-linking agent. Cross-linking is a stabilization process because it binds one polymer to another, forming a network structure where polymers can't move as a single chain.¹²⁴ The cross-linking agent we used during the 3D Modeling technique was 100mM Calcium Chloride (CaCl₂). According to Mikula et al., using calcium chloride as a cross-linking agent leads to greater structural integrity and increases the sorption capacity of hydrogels.¹²⁸

To summarize, alginate-gelatin hydrogels showed high functionality and effectiveness and may be good candidates for tissue modeling.

2.2.2 3D Modeling Technique

Confluent HT-29 and IRM-90 cells were washed with sterile PBS and detached using 0.25% trypsin (Gibco, Burlington, ON, Canada). A fresh culture medium was added. The culture medium was Dulbecco's modified Eagle's medium containing 4.5 g glucose/liter and supplemented with 10% Fetal Calf Serum (FBS) and penicillin/streptomycin (100 units/mL of penicillin and 100 µg/mL of streptomycin).¹¹⁸

Then the cells were centrifuged at 500 x g for 5 min, the supernatant medium was removed, the cell residue was prepared, and the cells were counted using the hemocytometer. The above experimental steps are the same steps described in the passaging procedure. After cell counting, we designed our experiment, as it is roughly illustrated in Figure 7. The cells were classified to form the following 3D Models: 3D Models consisting of the HT-29 cell line, 3D Models consisting of the IRM-90 cell line, and 3D Models including a co-culture of HT-29 and IRM-90 cell lines in different intestinal cells/fibroblasts ratios. The HT-29: IRM-90 Ratios that were chosen were 1:0.5, 1:1 and 1:2. The following experimental technique was done:

First, we removed the existing culture medium, washed the cells with sterile PBS, and detached them using 0.25% trypsin (Gibco, Burlington, ON, Canada). After a 3-minute incubation in trypsin solution at 37 °C in a humidified cell culture incubator with 5% CO₂, we collected the cell suspension and centrifuged at 500 x g for 5 min. After centrifugation, we removed the supernatant medium and diluted the cell residue with a 2ml growth medium mixing well with a pipette. We aspirated 15µl of the cell suspension and mixed it with 15µl Trypan Blue (ThermoFisher, ON, Canada). Then we applied the 30 µl solution to the edge of a hemocytometer and determined the number of fibroblasts per chamber by direct counting using a microscope. We calculated the concentration of cells in the original mixture using the formula:

Concentration of cells in the original mixture = [(number of cells counted x dilution factor) / number of chambers] x 10,000.

After calculating the total number of cells in the original mixture, we aspirated the appropriate amount of cell suspension, and we mixed it with A1G7 hydrogel, warmed in a 37 °C water bath. The estimated concentration was 1,000,000 cells/ml. We mixed the cell suspension with the hydrogel and applied the mixture in the wells of well plates. Therefore, 3D single-cell culture models were generated by adding 200,000 suspended cells (either HT-29 cells or IRM-90 cells) into 200µl A1G7 Hydrogel per well. Each 1:0.5 intestinal/fibroblast ratio co-culture model consisted of 200,000 HT-29 cells and 100,000 IRM-90 cells in 300µl Hydrogel; the 1:1 ratio model included 200,000 intestinal cells and 200,000 fibroblasts in 400µl A1G7 Hydrogel and the 1:2 intestinal/fibroblast ratio co-culture 3D model consisted of 200,000 HT-29 cells and 400,000 IRM-90 cells seeded into 600µl Hydrogel. After cell seeding, the crosslinking agent was added. According to Li et al., CaCl₂ 4mM was the appropriate Ca²⁺ level for improving hydrogel's physical and oxidative stability.¹²⁹ As a result, a layer was formed in each well. A sample of our models can be seen in Figure 8. All layers were covered with medium containing DMEM + 10% Fetal Bovine Serum (FBS) + 1% Penicillin-Streptomycin. Finally, the plate (seen in Figure 9) was kept inside the culture incubator to let the cultures grow. The growth medium was changed every 3 days.

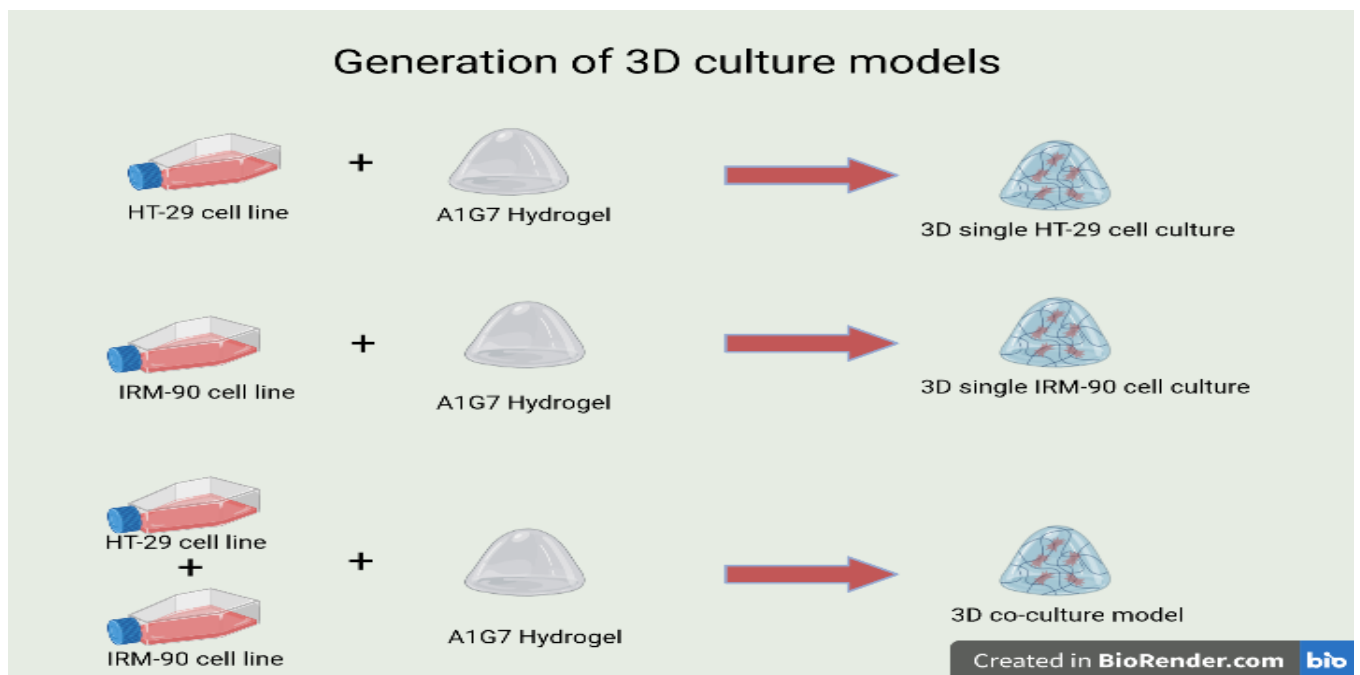


Figure 7- The procedure of generation of 3D culture model for single culture and co-culture

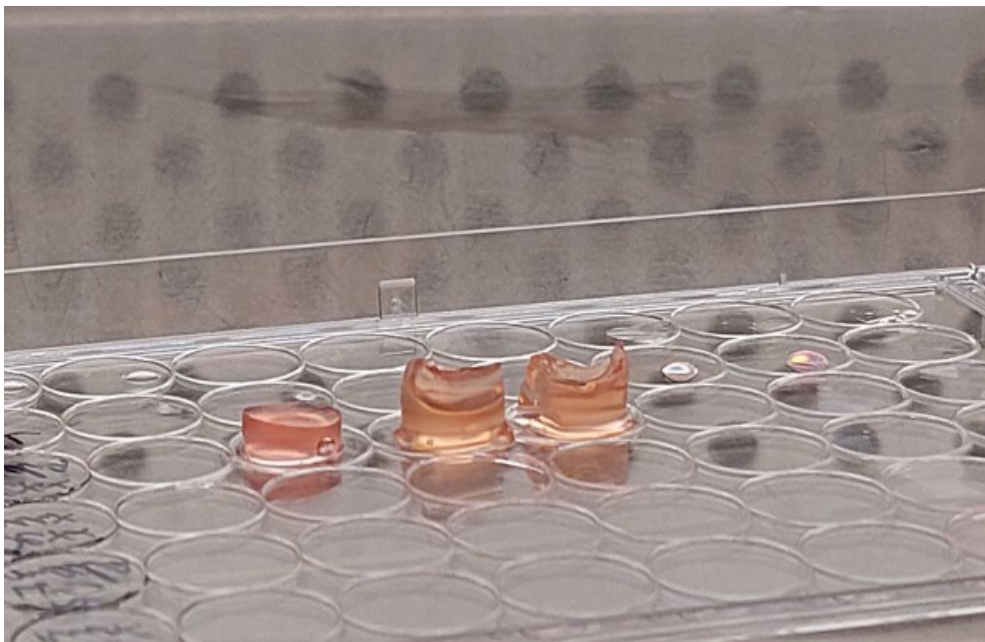


Figure 8- 3D models of single culture and co-culture



Figure 9- 3D Model culture plate

2.2.3 Evaluation Assays of the 3D single culture and co-culture system

Generation of the 3D single culture and co-culture system was followed by evaluation of the 3D Models with 3 evaluation Assays: The Alamar Blue Assay, the Viability/Cytotoxicity Assay, and the Cell Proliferation Assay. Of note, this experimental process took place 6 times.

Alamar Blue Assay is a metabolism-based method for monitoring cell function, cytotoxicity, and cell proliferation. It is a quantitative analysis method that detects the metabolic mitochondrial activity of cells fluorometrically and has been used for about 50 years.¹³⁰ The active ingredient is resazurin, which is water-soluble, non-toxic, non-fluorescent, and permeable through cell membranes. After entering living cells, the oxidized resazurin is reduced to resorufin, which is fluorescent. This electron reduction is translated to a color change from blue to pink.^{130,131} The more metabolically active the cells are, the more

fluorescent and pinker the reagent becomes. The advantages of this method are that the reagent is non-toxic and non-radioactive, the technique is easy to use, not labor intensive, and has a low cost.¹³⁰ The limitation of this method is that the metabolism analysis can be affected by cell number and cell metabolism. Also, it has been shown that fluorescence can be different depending on the incubation time. In addition, Munshi et al. found that the reagent can interact with the media regardless of the presence of living cells. This fact can lead to different fluorescence measurements.¹³² To avoid measurement discrepancies, it is suggested that the same cell number and incubation time be confirmed. Finally, there is a need for routine subtraction of the background fluorescence due to the interaction of the Alamar blue reagent with media-only samples.¹³²

Cellular metabolic activity was determined on days 1, 3, and 7. AlamarBlue™ assay (ThermoFisher) prepared in serum-free Dulbecco's Modified Eagle Medium according to manufacturer's instructions at 1:10 dilution. We added 300µL of the solution to each well, and we incubated the 3D Model Cultures for 6 hours at 37°C in a humidified cell culture incubator with 5% CO₂. Afterward, we took 100µL of the above solution from each well, and the samples' fluorescence was measured in 96-well plates using a Tecan M200 Pro plate reader (Tecan, Männedorf, Switzerland). Fluorescence excitation was 540nm, and fluorescence emission was 590nm. Fluorescence was measured in Relative Fluorescent Units (RFU).

Viability/Cytotoxicity Assay (Live/Dead Assay®) is a two-color assay to determine cell viability based on intracellular esterase activity and plasma membrane integrity. The kit contains calcein-AM, which stains live cells, and Ethidium Heterodimer, which stains dead cells. Green-fluorescent calcein-AM indicates intracellular esterase activity, an enzyme responsible for prodrug activation and detoxification. On the other hand, Ethidium

Heterodimer is a red-fluorescent dye that is membrane-impermeable, and it can enter only dead cells through the disrupted membrane and bind to DNA.

The solution used for LIVE/DEAD® Assay (Invitrogen, Carlsbad, CA, USA) consists of 10 μ L of calcein and 20 μ L of Ethidium Heterodimer in 10mL Phosphate Buffer Saline Buffer (PBS; ThermoFisher, Waltham, MA, USA). After 7 days of culture, we added 200 μ L of the above solution to each 3D Model well and incubated for 30 minutes at room temperature. Afterward, we washed the hydrogel models with PBS, took a small representative sample, and placed it on a glass slide. We used fluorescent microscopy to count the percentage of live cells compared to dead cells. An Olympus IX81 inverted fluorescence microscope using a 10x objective with MAG Biosystems Software 7.5 (Photometrics, Tucson, AZ, USA) was used to capture images at 10X magnification. After taking at least 3 photo captures from each slide, we counted the number of live cells that appear green in color and the number of dead cells that appear red in color. Then we calculate the average percentage of live cells on each slide.

The last evaluation assay used was the Hoechst Assay for cell proliferation assessment. Following 7 days of culture, 3D models were gently rocked in 500 μ L of 4M guanidine hydrochloride (GuHCl) buffer for 48 hours at 4 °C. DNA content for 3D single cell and 3D co-culture models was measured using DNA Hoechst 33258 assay. All GuHCl extracts were diluted 10-fold before analysis. The adenine-Thymine (AT) content of a DNA sample affects the Hoechst 33258- DNA fluorescence, so we tested the samples using a similar standard. Calf-thymus DNA (Invitrogen, Carlsbad, CA, USA) is used as a reference because it's double-stranded, highly polymerized, and is approximately 58% AT (42% GC). Calf-thymus DNA supplemented with the same 0.4M GuHCl as the samples were used to generate the standard curve. Hoechst 33258 (Molecular Probes, ThermoFisher, Burlington, ON, Canada) was prepared according to the manufacturer's instructions (ThermoFisher). The samples

were analyzed in triplicate, using a Tecan M200 Pro plate reader (Tecan, Männedorf, Switzerland), at 352nm excitation and 460nm emission, and 420 nm cut-off. Standard curves were generated on the worksheet to interpolate sample DNA quantity.

2.3 Objective 2- Modeling IBD with the 3D co-culture system

After 3D Model generation and Evaluation with metabolic activity assay, cell viability assay, and cell proliferation assay, a 3D co-culture model was generated using intestinal cells and IRM-90 fibroblast cells in a cell ratio 1:0.5. Modeling IBD was the next step of our project. This step included the induction of 3D inflammation followed by treatment with anti-inflammatory factors. Both situations were assessed for model inflammation response by measurement of protein concentration of Tumor Necrosis Factor α (TNF α) and Interleukin 1 β (IL-1 β) in collected culture media. Both cytokines are pro-inflammatory cytokines involved in the initial inflammation pathway of IBD pathophysiology. Concerning cancer cells, it is known that TNF α is also a pro-inflammatory cytokine that promotes tumorigenesis. However, IL-1 β is still unclear in tumorigenesis but is known to be involved in cancer cell function.¹¹⁵

2.3.1 Factors that induce inflammation

Mediators of inflammation are substances that initiate and regulate inflammatory reactions. They are cell-derived or plasma protein-derived vasoactive amines, lipid products, cytokines, and complement activation products. There are different experimental models for studying inflammation and inflammatory disease. The most commonly used models are the chemically induced inflammation models, including the dextran sodium sulfate (DSS) mouse model,¹³³ oxazolone-induced colitis model, lipoteichoic acid¹³⁴, TNBS-induced colitis model, and experimental models using Lipopolysaccharide (LPS). Some of these

inflammatory agents, such as DSS and TNBS, have been used for establishing experimental animal models of Ulcerative Colitis.¹³⁵

Dextran Sulphate Sodium (DSS) is a water-soluble polysaccharide that induces intestinal inflammation in experimental animal models. Although the DSS-colitis model is widely used due to its rapidity, simplicity, and reproducibility, a significant limitation is that the development of colitis isn't characterized by T and B cell activation, like human colitis.¹³³

Oxazolone is a chemical compound that induces oxazolone-colitis that is a Th2 inflammation, and resembles Ulcerative Colitis. Although it is a good study model, it isn't identical to the human UC.¹³⁶ Lipoteichoic acid (LTA), an inflammatory bacterial molecule located in the cytoplasmic membrane of Gram-positive bacteria. LTA can induce inflammation by secreting molecules which activate host macrophages, but it is considered less active than other inflammatory factors.¹³⁴ 2,4,6-trinitrobenzene sulfonic acid (TNBS) is an oxidizing acid that induces delayed hypersensitivity reactions, but it has been used in mice models to induce TNBS colitis. A T cell-mediated immune response characterizes the mice colonic mucosa exposed to TNBS.¹³⁷ However, TNBS-colitis doesn't recapitulate IBD etiopathogenesis, and TNBS-colitis can't be used as a study model.¹³⁸

Lipopolysaccharide (LPS) is an inflammatory agent, an endotoxin derived from a Gram-negative bacterial cell wall. According to the literature, LPS stimulates both the immune system and epithelial cells, and the effects of LPS have been studied on macrophages, T-lymphocytes, as well as intestinal epithelial cells, including the HT-29 cell line.^{139,140} The interaction between LPS and host cells is mediated by Toll-like Receptor 4 (TLR4), a receptor for LPS and expressed on the cell surface of hematopoietic and endothelial cells.¹⁴¹ TLR4 initiates an intracellular pathway, leading to the transcription of pro-inflammatory cytokines, such as IL-1 β and TNF α .^{141,142} Based on this knowledge, experimental LPS models recapitulate this inflammatory process because shortly after LPS

administration, pro-inflammatory cytokine levels (i.e., TNF α) are increased and can be measured in circulating serum. Compared to the other inflammatory factors, LPS was chosen because of its technical ease and high reproducibility. In addition, the increase in pro-inflammatory cytokines is observed shortly, within 48 hours, after LPS administration.

2.3.2 Inducing and suppressing inflammation – experimental process

During our experiment, we treated the co-culture model with LPS in a concentration of 100 ng/ml according to existing literature experiments.¹⁴³ The culture medium used contained Dulbecco's modified Eagle's medium with 1% Fetal Calf Serum (FBS) and penicillin/streptomycin (100 units/mL of penicillin and 100 μ g/mL of streptomycin). We treated the co-culture models in two ways to study potential different inflammatory responses. In group 1, we mixed LPS and seeded cells with the A1G7 Hydrogel and collected the culture medium after 48-hour incubation. In group 2, we let our co-culture model be incubated for 24 hours, and then we treated them with an LPS-containing medium. Afterward, we collected the culture medium after 28-hour incubation. Finally, we used a 3rd model group as the control group, where no LPS was added.

The second part of IBD modeling with our 3D co-culture system was to assess the model response to anti-inflammatory factors, so we used dexamethasone. Dexamethasone is a synthetic glucocorticoid, and it has been shown for decades to inhibit inflammation and the expression of cytokines TNF- α and IL-1 β .¹⁴⁴ In a recent study was demonstrated that dexamethasone (molarity of 1 μ M or 10 μ M) inhibits LPS-induced TNF- α secretion in activated macrophages.¹⁴⁵ In our experiment, the culture medium consisted of DMEM with 1% Fetal Calf Serum (FBS) and penicillin/streptomycin (100 units/mL of penicillin and 100 μ g/mL of streptomycin). We treated our model with LPS accompanied by Dexamethasone

10 μ M, which had a more significant anti-inflammatory response, according to Chuang et al. At this time, we added two more 3D model groups compared to the LPS treatment experiment. In one group, LPS and Dexamethasone were mixed with the cells, and then the cells were seeded into A1G7 Hydrogel. In the other group, we incubated the 3D co-culture models for 24 hours. We added LPS in concentration 100ng/ml and incubated the LPS-treated models for 2 hours to let them respond to inflammation.¹⁴⁵ Afterwards, the co-cultured cells were treated with dexamethasone 10 μ M. After 48 hours of incubation, the culture medium was collected, and cytokine expression was assessed using ELISA.

2.3.3 Evaluation of model response to inflammation and anti-inflammatory factors

Cytokine measurement was done by using Enzyme-Linked Immunosorbent Assay (ELISA) kits (RayBiotech, Peachtree Corners, GA, USA) according to the manufacturer's instructions. ELISA is an immunological assay to detect antibodies, antigens, proteins, and glycoproteins. The ELISA assay used was a sandwich enzyme immunoassay technique. A monoclonal antibody specific for human TNF α or IL-1 β has been pre-coated onto a microplate. Standards and samples are added to the wells, and any cytokine of interest present is bound by the immobilized antibody. After washing away any unbound substances, an enzyme-linked polyclonal antibody specific to the studied cytokine is added to the wells. Following a wash to remove any unbound antibody-enzyme reagent, a substrate solution is added to the wells, and color develops in proportion to the amount of the cytokine bound in the initial step. The color development is stopped, and the intensity of the color is measured.¹⁴⁶ Results are displayed in the Excel sheet. After using the equation of the standard curve, we calculated the TNF- α or IL-1 β concentration (pg/ml). We compared the results between the LPS-treatment group, the LPS-Dexamethasone-treatment group, and the control group.

2.4 Statistical analysis

All experiments were repeated at least three times (N=3), and measurements were performed in triplicates (n=3). Results are expressed as mean \pm SD. All statistical analyses were performed using unpaired t-tests from at least three independent experiments. We compared the 3D model results to the control, LPS-treated models to control groups, and Dexamethasone-treated models to LPS-treated models. Significance was set at $p < 0.05$. Analyses were performed using Microsoft Excel.

CHAPTER 3

RESULTS

3.1 3D Model Characterization

The generated 3D Models, incubated in a 48-well plate, included 3D single-culture and 3D co-culture models. The 3D single culture models consisted either of HT-29 cells seeded in 200 μ L of A1G7 Hydrogel or IRM-90 cells seeded in 200 μ L of A1G7 Hydrogel. The 3D co-culture model consisted of a mixed HT-29 cell line and IRM-90 cell line in ratios 1:0.5, 1:1, or 1:2. The co-culture was also seeded in 200 μ L of A1G7 Hydrogel. The 3D models had a diameter of 9.8mm and height of 5 ± 2 mm for the single culture and 10 ± 2 mm for the co-culture. Figures 10 and 11 demonstrate our models' appearance under the optical microscope.

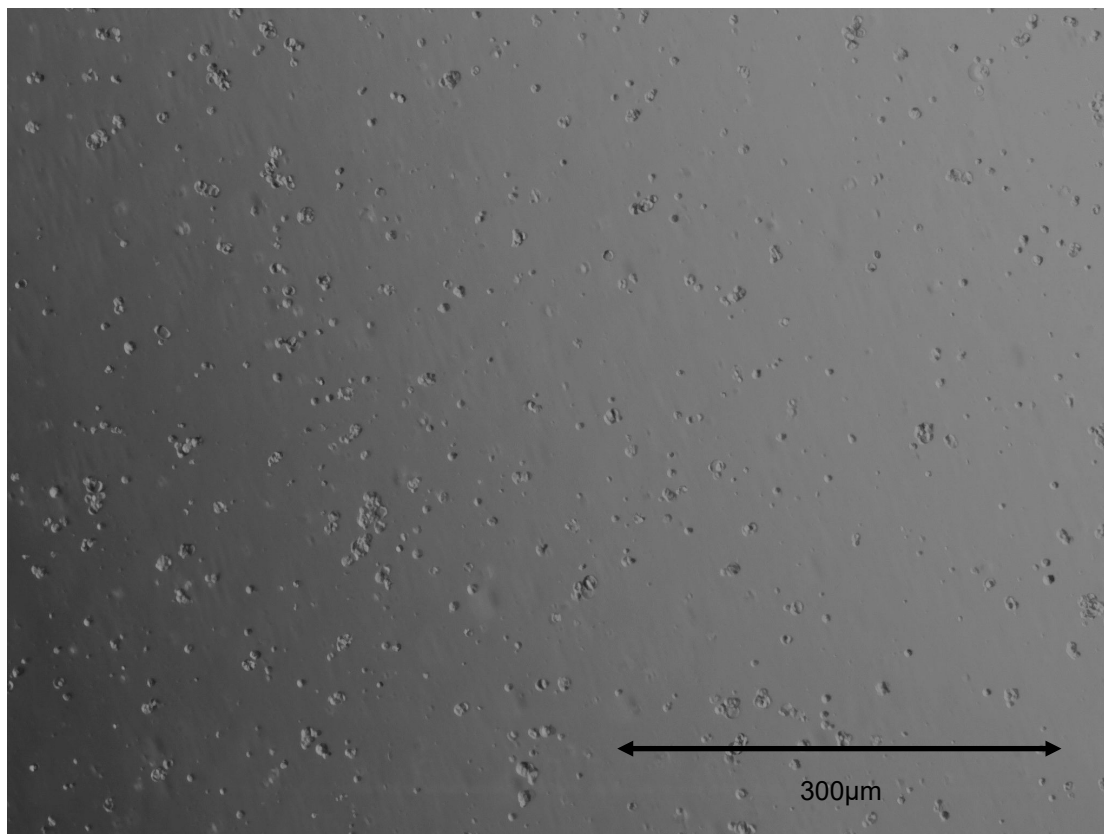


Figure 10: 3D HT-29 cell culture model

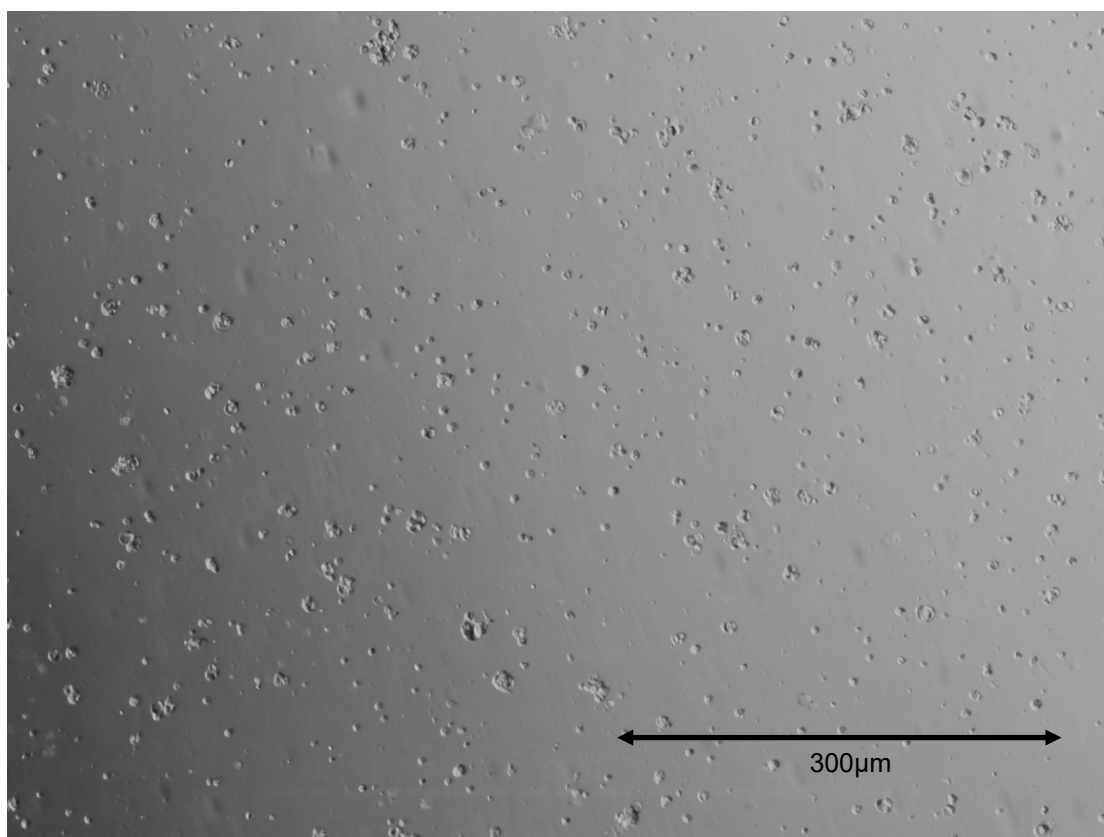


Figure 11: 3D 1:0.5 co-culture model

3.2 Cell metabolic activity

Cell metabolic activity for all cell-seeded 3D Models was measured with AlamarBlue™ assay. Fluorescence was measured in Relative Fluorescent Units (RFU) on days 1, 3, and 7. The control group included wells with no 3D Models. Figure 12 demonstrates that 3D HT-29 cell culture models developed a progressively increased metabolic activity, that was, on average, approximately 20,000 RFU (± 3993) on day 7. On the other hand, IRM-90 fibroblasts were more active with a measured fluorescence at 28,000 RFU (± 5289) on Day 1, and the activity reached a plateau on Days 3 and 7 (average OD was approximately at 30,000 RFU ± 5127). Concerning the 3D co-culture models, the metabolic activity was high for all co-culture ratios, and it reached on Day 7 an average fluorescence measurement of approximately 30,068 (± 3331) RFU for 1:0.5 ratio co-culture, 28,808 (± 2608) RFU for 1:1 ratio co-culture, and 30,719 (± 6009) RFU for 1:2 ratio co-culture. Notably, a progressive increase in metabolic activity was observed in the 1:0.5 ratio co-culture model, whereas the other 3D co-culture models plateaued their activity on days 3 and 7. All 3D Models displayed significantly higher metabolic activity compared to control group as showed in Figure 12 ($p < 0.01$ and $p < 0.05$).

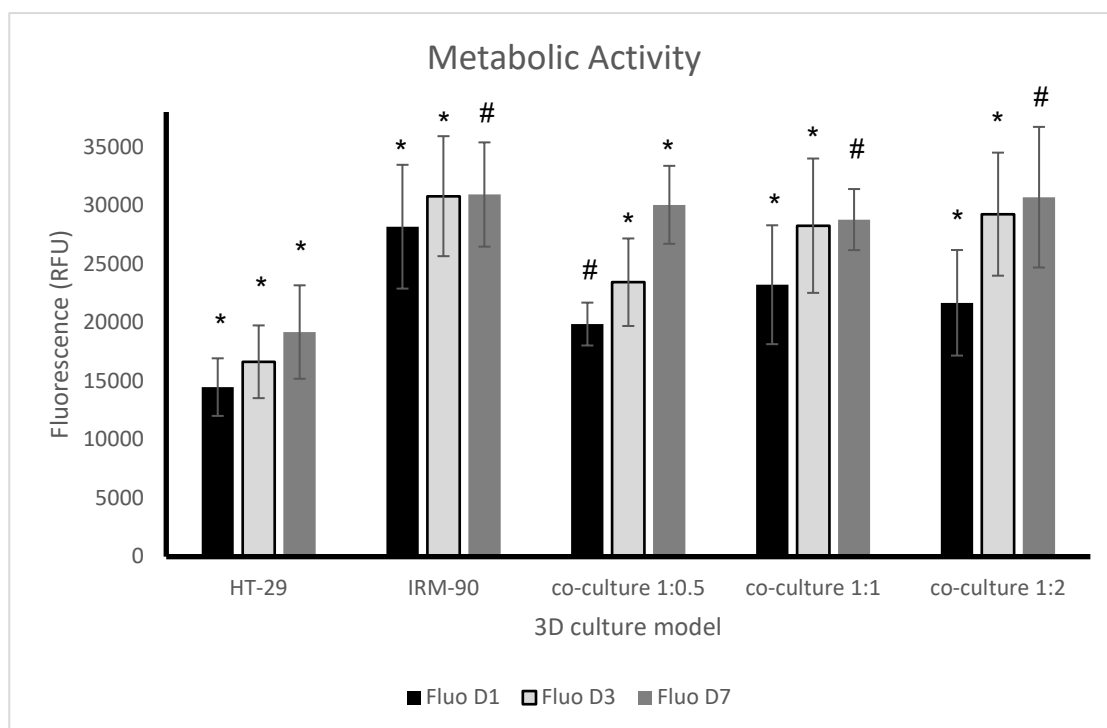


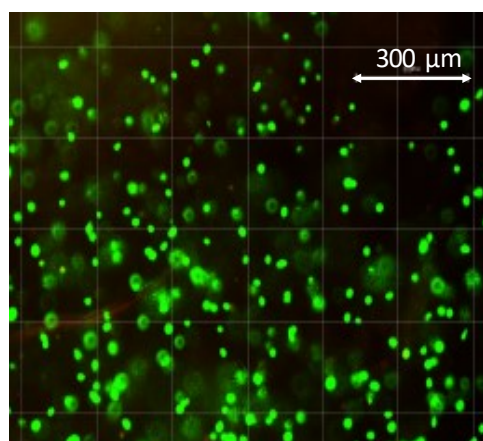
Figure 12: Metabolic Activity quantified via AlamarBlue™ assay at days 1, 3, and 7 of culture. After a specific incubation time (6 hours), we measured the fluorescence of the dye added to 3D models and compared it to the fluorescence of the dye added to empty (control) wells. There was statistical significance in metabolic activity between the model and control groups. * = $p < 0.01$ and # = $p < 0.05$. Error bars represent \pm SD.

3.3 Cell viability

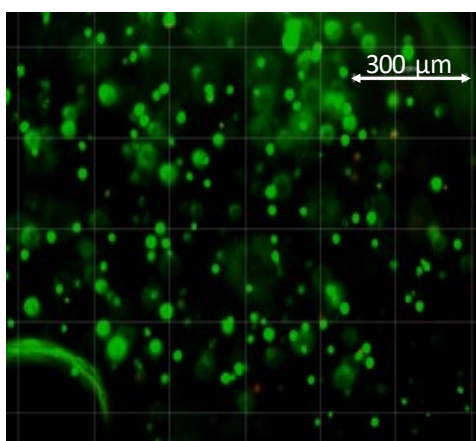
Cell viability was assessed with Live/Dead™ assay (Figures 13 - 15). Representative images demonstrate that the number of dead cells in 3D single-culture models and 3D co-culture models was negligible in all cases.

The estimated percentage of intestinal cells on days 1, 3 and 7 was $87.9 \pm 2.21\%$, $91.1 \pm 3.74\%$, and $95.4 \pm 2\%$, respectively, and the estimated rate of live fibroblasts cells on days 1, 3 and 7 was $86.0 \pm 3.25\%$, $90.6 \pm 3.29\%$, and $92.4 \pm 2.47\%$, respectively. (Figure 16). Concerning the co-culture models, the percentage of live cells on day 7 was also high ($93.7-96\%$), regardless of the co-culture ratio. (Figure 17).

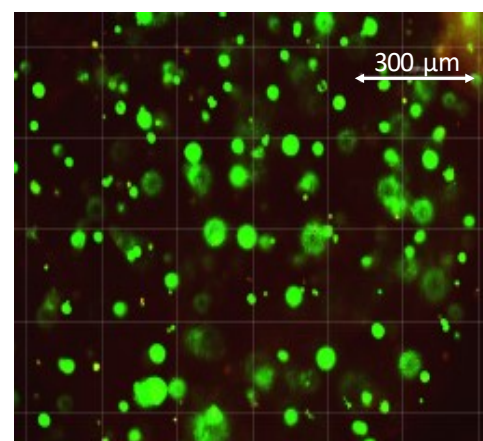
3D HT-29 cell culture models



Day 1

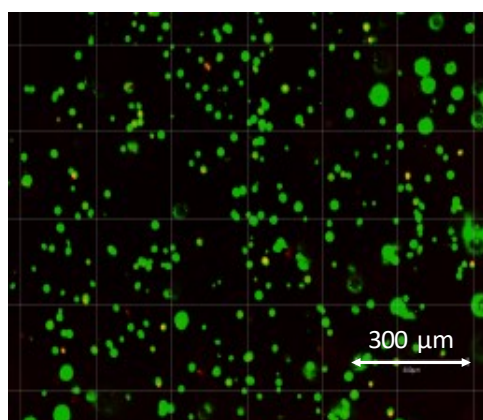


Day 3

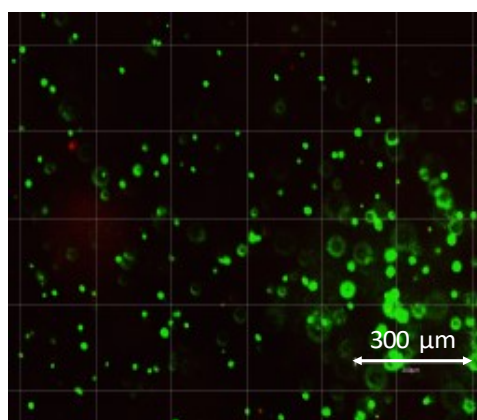


Day 7

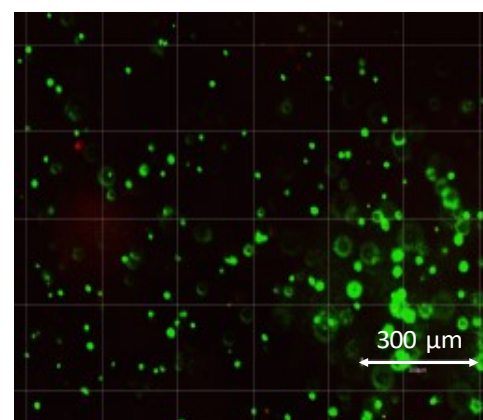
3D IRM-90 cell culture models



Day 1



Day 3



Day 7

Figures 13 and 14: Florescence microscopy images representing 3D HT-29 cell culture models (upper row) and 3D IRM-90 cell culture models (lower row) on Days 1, 3, and 7. The percentage of live cells (green-fluorescent cells) is significantly higher compared to dead ones (red-fluorescent cells).

Viability assay for co-culture - Day 7

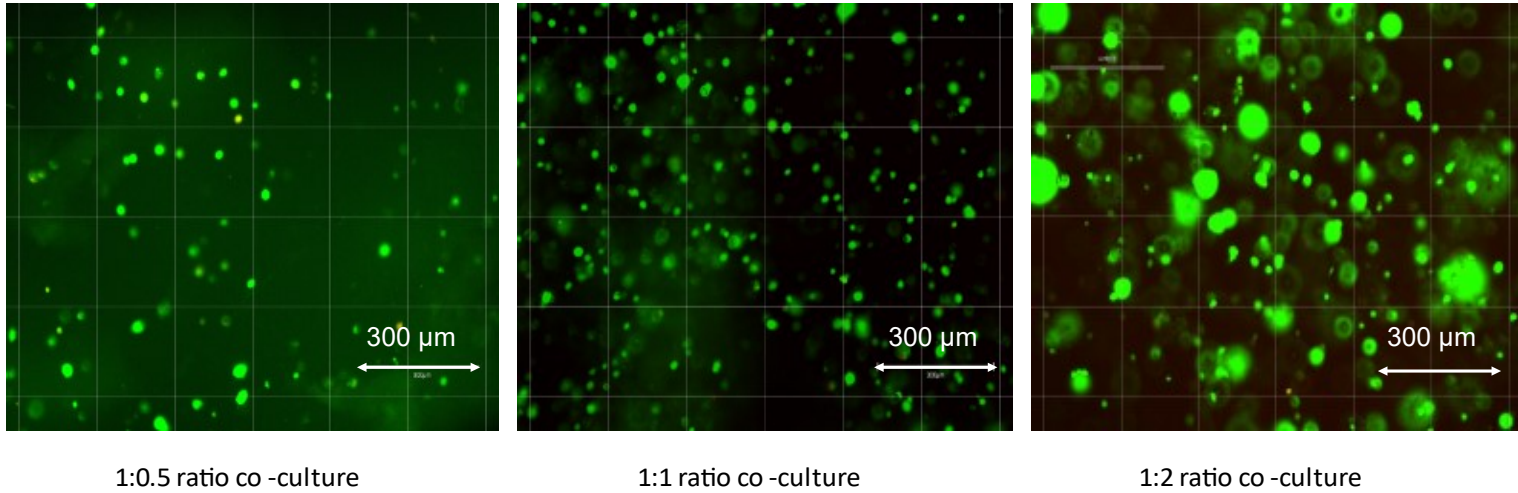


Figure 15: Fluorescence microscopy images representing the following 3D culture models on Day 7: 3D 1:0.5 ratio co-culture model (left), 3D 1:1 ratio co-culture model (middle), 3D 1:2 ratio co-culture model (right).

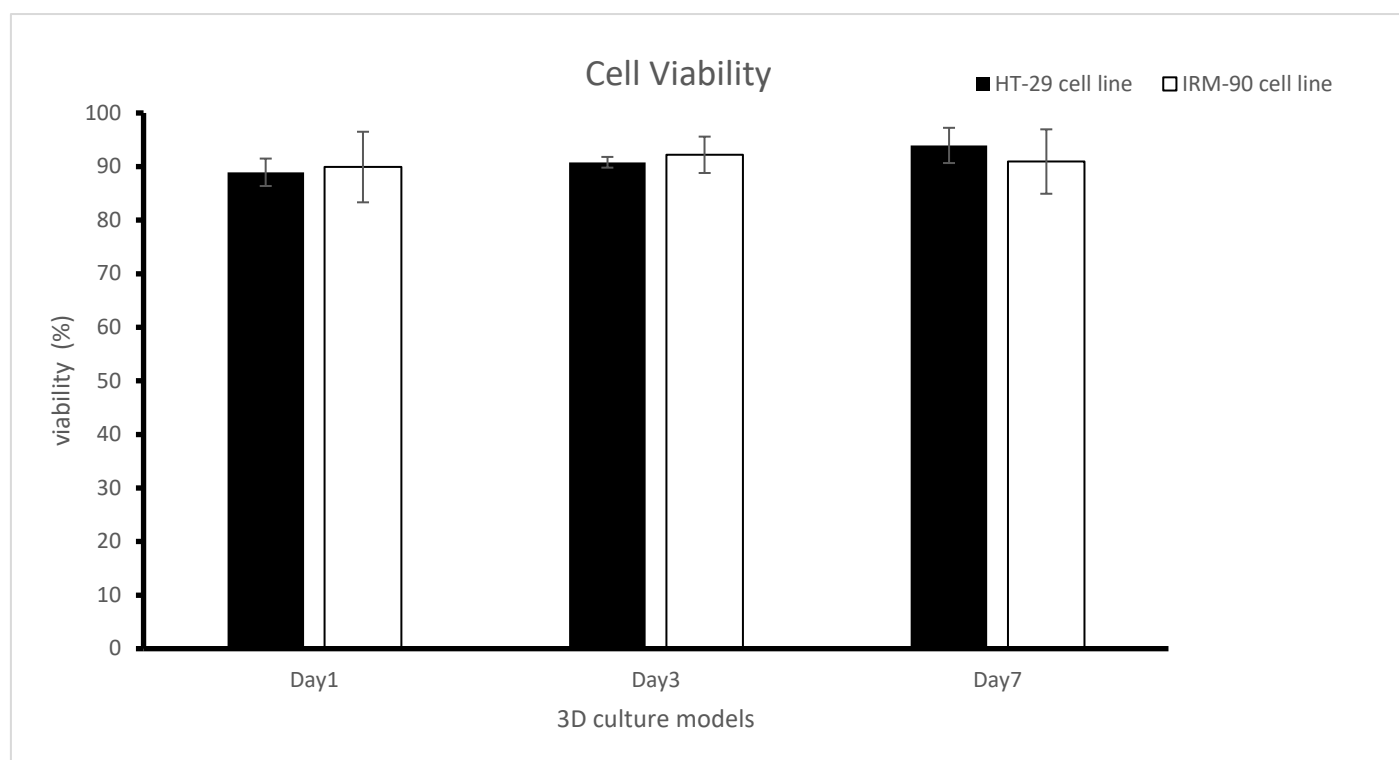


Figure 16: 3D-model cell viability quantified via Live/Dead™ assay at days 1, 3, and 7 of culture. Our 3D Model supports cell viability during the whole experiment. Error bars represent \pm SD.

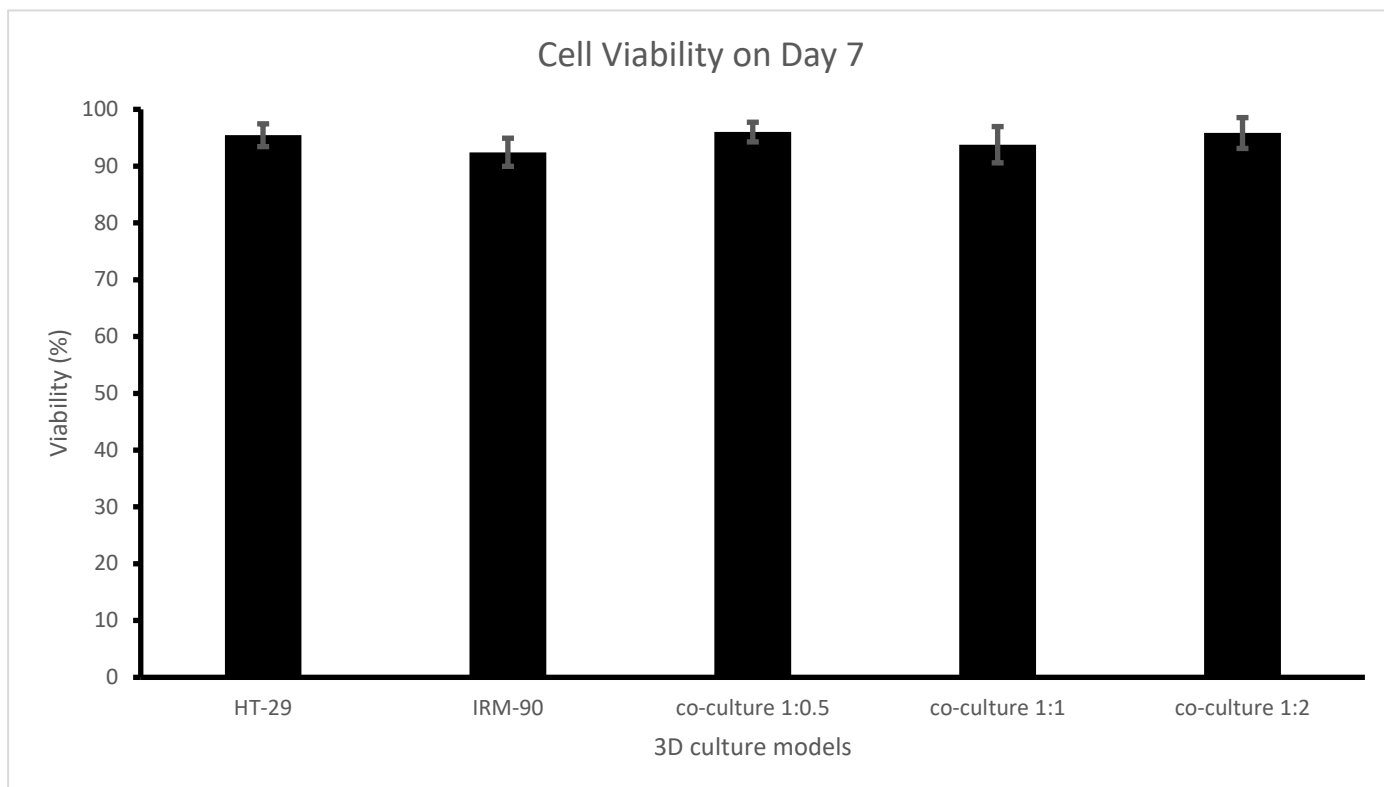


Figure 17: 3D-model cell viability quantified via Live/Dead™ assay after 7 days of culture. All 3D Models support high percentage of live cells after 7 days of culture. Error bars represent \pm SD.

3.4 Cell proliferation

To confirm whether the increased metabolic activity for the various 3D models was due to cell growth, cell number increase at 7 days was assessed by Hoechst assay. As Figure 18 shows, the initial cell number for single-cell culture models was 200,000 cells, and the measured cell number for the HT-29 cell line and IRM-90 cell line was 716,037 (\pm 76.9) cells and 332,477 (\pm 33.7) cells, respectively. Concerning the intestinal: fibroblast co-culture models, the seeded intestinal cells on day 0 were 200,000, and the fibroblast cells were

used in ratios 1:0.5, 1:1, and 1:2. At the end of day 7, co-culture cells were measured to 814,387 (± 20.48) cells for ratio 1:0.5, 545,282 (± 29.42) cells for ratio 1:1 and 1,333,429 (± 101.9) cells for ratio 1:2. (Figure 18). Then, we estimated the per fold cell number increase for each 3D model based on the estimated cell number on Day 7. We used the percent increase formula ($\% \text{ increase} = \text{Increase} \div \text{Original Number} \times 100$). HT-29 cell culture model showed a 3.5-fold increase, and IRM-90 cell culture model showed a 1.6-fold increase. The 3D co-culture models also supported cell proliferation since the cell proliferation rates were 2.7-fold, 1.3-fold, and 2.2-fold for ratios 1:0.5, 1:1, and 1:2, respectively. (Figure 19). The conclusion is that the 3D 1:0.5 co-culture model had a higher proliferation rate.

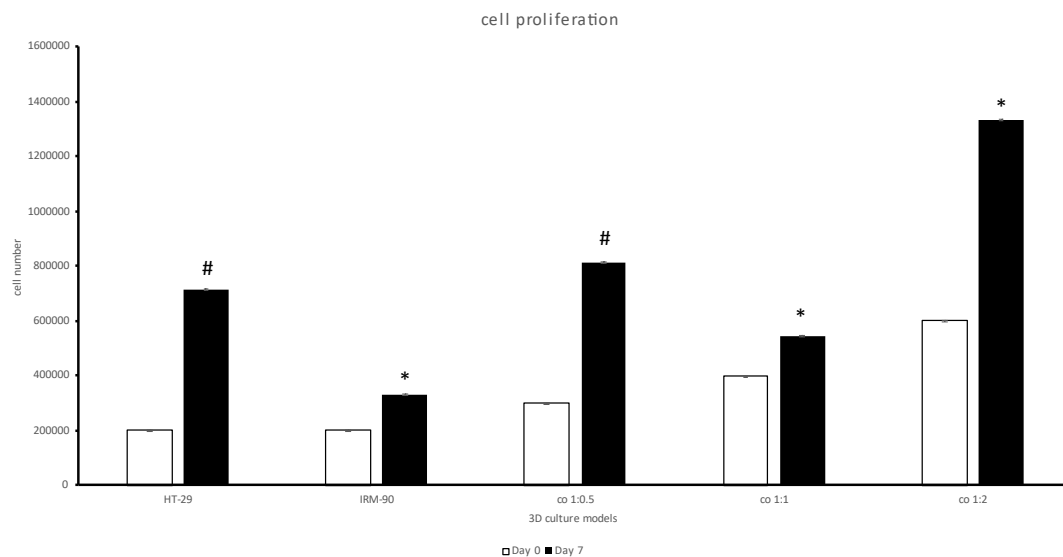


Figure 18: 3D-model cell proliferation quantified via Hoechst™ assay at day 7 of culture. Error bars represent \pm SD. SD value was significantly low. For the p-value: * = $p < 0.01$ and # = $p < 0.05$

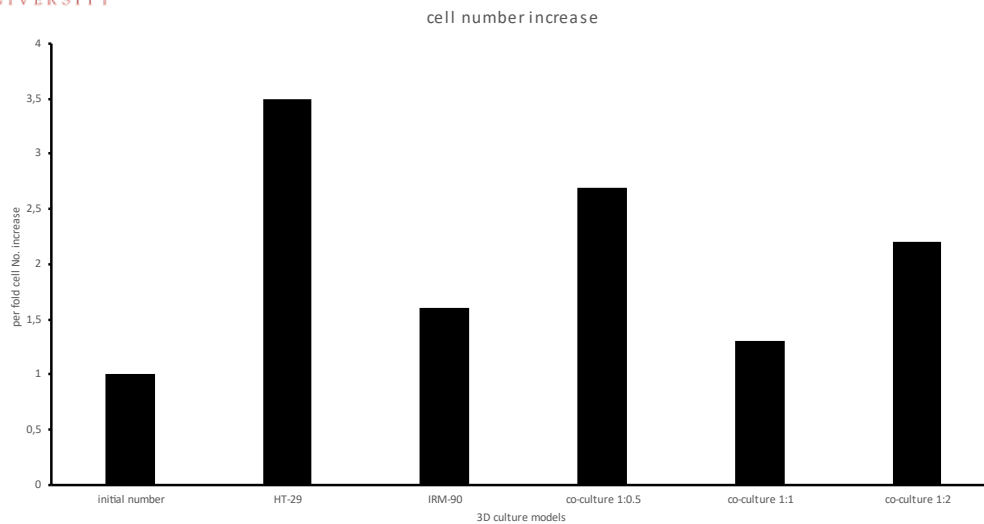


Figure 19: Cell proliferation rates of the 3D single culture and 3D co-culture models. Based on the estimated cell number on Day 7, we calculated the percentage cell number increase for each model.

3.5 Cytokine expression

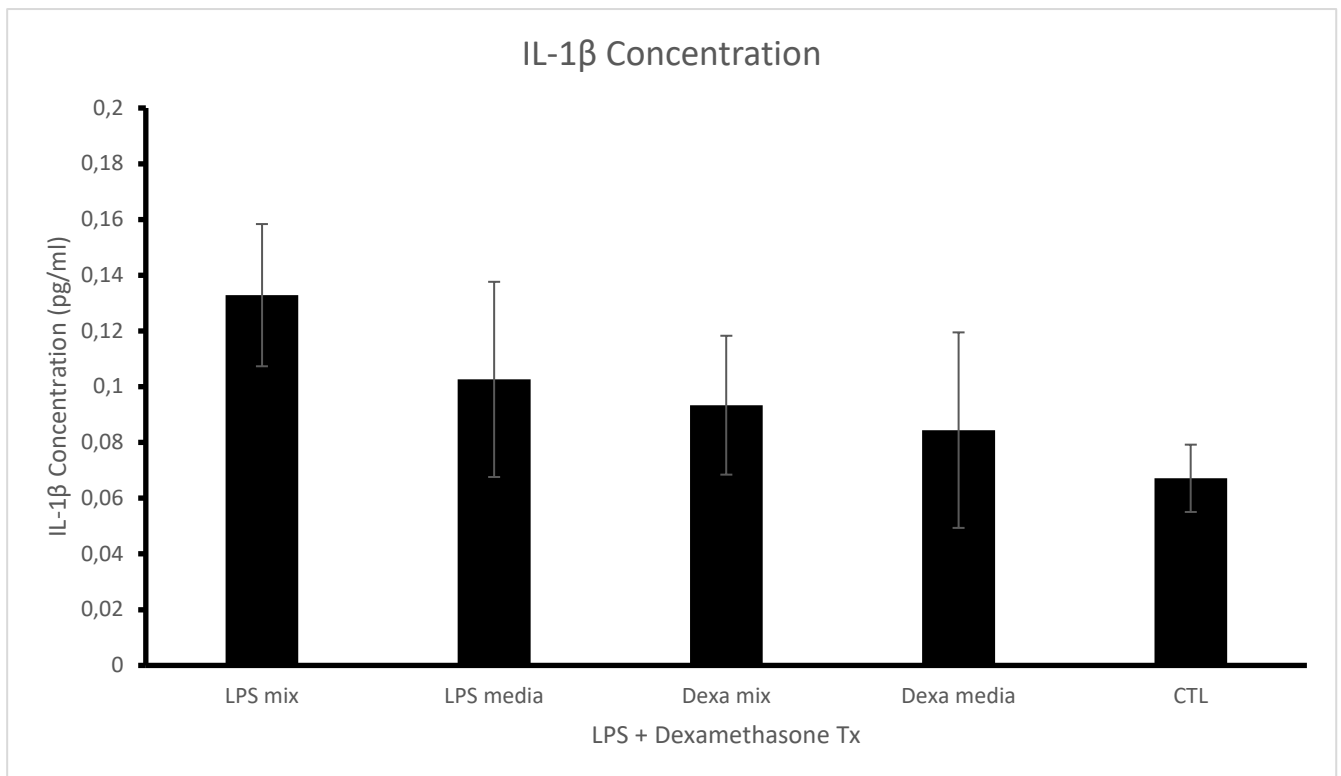
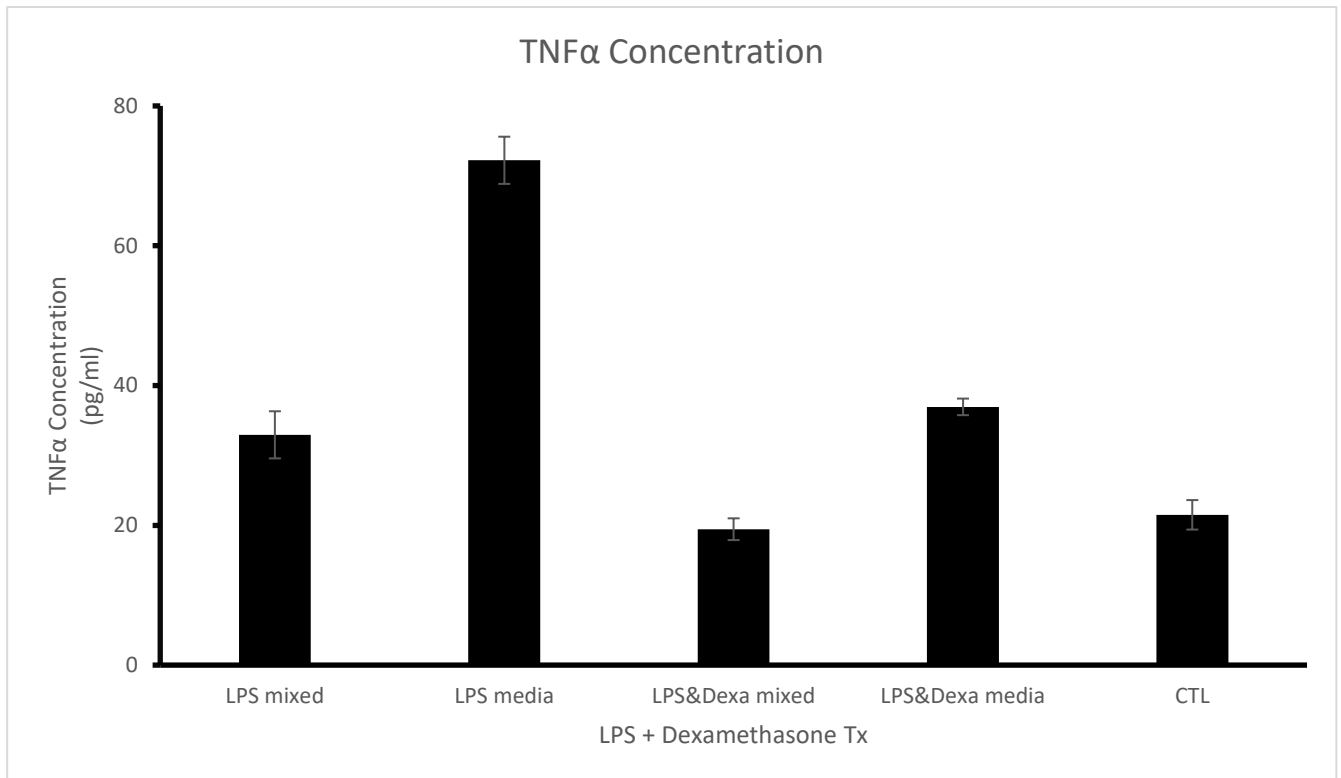
3D Model response to inflammation was assessed by ELISA assay. Cytokine expression of TNF α and IL-1 β was measured in models treated with LPS and in models of the control group (without LPS treatment). There were three model groups; Group 1 included 3D models in which LPS was mixed with cell-seeded hydrogel. Group 2 had 3D models in which LPS was added to the culture medium after 24 hours of incubation. Group 3 was the control group which included models without LPS.

TNF α concentration in group 1 was 32.94 ± 3.37 pg/ml, and TNF α concentration in group 2 was 72.2 ± 3.38 pg/ml, whereas the TNF α concentration in the control group

was measured at 21.5 ± 2.11 pg/ml. This concentration change is translated into a 53.2% increase in TNF α concentration when LPS was mixed with the cells and a 235.8% increase in TNF α concentration when LPS was added to the culture medium. (Figure 20)

The ELISA results for IL-1 β were a little different. IL-1 β concentration in group 1 was 1.13 ± 0.03 pg/ml, 0.10 ± 0.04 pg/ml for group 2, and 0.067 ± 0.01 pg/ml for group 3. These results are translated into a 94.02% increase in IL-1 β concentration when LPS was mixed with the cells and a 49.2% increase in IL-1 β concentration when LPS was added to the culture medium. (Figure 21)

After adding Dexamethasone to the inflamed 3D models, the cytokine expression results were the following. The TNF α Concentration was decreased to 19.44 ± 1.56 pg/ml when Dexamethasone (Molarity= 100 μ M) was mixed with the containing LPS 3D co-culture models. In addition, TNF α Concentration was decreased to 36.94 ± 1.19 pg/ml when Dexamethasone was added to the culture medium after a 2-hour model incubation with LPS (Figure 20). The above changes are translated to a 41.10% decrease in TNF α expression for group 1 and a 48.84% decrease in TNF α expression for group 2 compared to the “inflamed” 3D models. Concerning the IL-1 β expression, the ELISA results showed that mixing dexamethasone with the inflamed cells leads to IL-1 β Concentration = 0.093 ± 0.02 pg/ml. Finally, IL-1 β Concentration was 0.084 ± 0.04 pg/ml when dexamethasone was added to the culture medium. The results above correspond to a 29.54% decrease in IL-1 β expression after mixing Dexamethasone with the model compared to cytokine expression after LPS treatment. The IL-1 β expression was decreased by 17.65% after adding dexamethasone to the culture medium. (Figure 21)



Figures 20 and 21: TNFα and IL-1β cytokine expression quantified by ELISA assay in 3D models mixed with LPS (group 1), in 3D models containing LPS in culture media (group 2), in 3D models mixed with LPS + Dexamethasone (group 3), in 3D models

containing LPS + Dexamethasone in culture media (group 4), and 3D models containing neither LPS nor Dexamethasone (control group). The culture medium was collected after 48 hours of incubation. Cytokine expression was assessed by ELISA assay. There was statistical significance in cytokine expression between groups exposed to inflammatory factor (LPS), groups treated with anti-inflammatory factor (Dexamethasone), and the control group. ($p < 0.005$).

CHAPTER 4

DISCUSSION

Due to IBD clinical course and IBD complications, there is a need for personalized medicine and novel therapeutics to control intestinal and extra-intestinal inflammation. The existing animal models, such as those genetically or chemically induced, present differences in anatomy, intestinal metabolism, and immune responses, and thus they do not exactly recapitulate the human disease.¹⁴⁷ In addition, there are other limitations, including the difficulty in using large multiplex arrays for drug screening and the ethical concerns of using animals in research.⁹⁵ On the other hand, the current *in vitro* 2D models do not allow the physiologic representation of the human tissue.¹⁰⁰ Furthermore, the co-culture of different cell types is not feasible in 2D models, so cell-to-cell communication and morphogenesis cannot be studied. Due to the limitations of the current experimental models to study the intestine, there is a growing interest in tissue engineering. An *in vitro* 3D organotypic culture can generate a bio-mimetic

physiological gut model using organoids. 3D culture models consist of primary tissue cells, embryonic stem cells, or induced pluripotent cell lines.¹⁴⁸ Intestinal organoids can self-renewal and self-organization and simulate the origin tissue. According to the literature, it has been proven that generating a 3D co-culture model is feasible, and a crypt-pattern structure formation promotes cell differentiation and renewal, recapitulating *in vivo* colon.¹⁴⁷ This study's results showed that the 3D co-culture model is responsive to inflammation and anti-inflammatory factors, indicating that organoids could be used as a screening platform for personalized medicine.

4.1 Cell types and hydrogel type

3D co-culture models with IBD patient-derived intestinal cells could contribute to the innovative approach to personalized medicine. Nevertheless, we performed the initial step of the *in vitro* studies using the HT-29 cell line derived from colorectal cancer. We chose this cell line because it is highly proliferative, relatively easy, and cheap. HT-29 cells can also respond to LPS and secrete inflammatory factors like those in IBD, like TNF α .³⁷ They are also very useful for assay and high throughput screening approaches.¹⁴⁸

The other 3D co-culture component was the IRM-90 cell line which is a normal human lung-origin cell line of fibroblasts, and their morphology and function might differ depending on the *in vivo* location.¹¹⁹ A recent study claims that fibroblasts can support intestinal epithelial cell growth by secreting growth factors such as Wnt and epidermal growth factor (EGF). They can also deposit collagen contributing to matrix composition

and colon organoid formation.¹⁴⁷ Finally, including fibroblasts in colon organoid formation supports vasculature formation as well.¹⁴⁷

Hydrogel is often used as the *in vitro* Extracellular Matrix (ECM) and plays a major role in 3D model formation. In general, hydrogels such as alginate and hyaluronic acid can support organoid growth with their high-water content, which promotes nutrient diffusion. Moreover, its flexibility and elasticity are similar to ECM, providing biochemical and structural support to the seeded cells.¹⁴⁹ Choosing the appropriate material for the hydrogel matrix is crucial. Among the existing options mentioned previously, we chose the natural hydrogels alginate and gelatin because combining these materials promotes advantages such as biocompatibility and mechanical properties. Furthermore, combining the above material overcomes several drawbacks, such as alginate's mechanical weakness and gelatin's quick biodegradation.¹⁴⁹ Finally, the chosen hydrogel is characterized by high reproducibility, supporting the experimental process.

Choosing the above cell types and matrix materials, which were easy to handle, made the 3D model generation repeatable and effective. The evaluation of the 3D single cell culture and co-culture models was done by the AlamarBlue Assay, the Live/Dead Assay, and the Hoechst Assay. The AlamarBlue Assay results showed high metabolic activity during the whole experiment. The intestinal culture model showed a progressive increase in metabolic activity, whereas the fibroblast model had a plateau in metabolic activity after day 3. The metabolic activity of 3D co-culture models was increased from 1.3 to 1.5-fold (depending on the cell ratio). Regarding the 3D culture cell viability, the Live/Dead Assay results showed that all our 3D models support cell growth. When we used fluorescence microscopy to assess the percentage of live cells in our models, we estimated cell viability over 92% on Day 7. Finally, we evaluated the

cell proliferation rate by comparing the initial number of the seeded cells to the cell number on Day 7. We found that all our models support cell proliferation, and we confirmed that the model's high metabolic activity was due to cell growth. When we estimated the per fold cell number increase, we found that the 1:0.5 intestinal/fibroblast cell culture ratio showed the highest cell proliferation rate. Of note, the estimated ratio of epithelial cells to pericryptal fibroblast sheath was 6.5:1,¹⁵⁰ but we chose the 1:0.5 ratio for our 3D co-culture model for technical ease and because of the high increase in cell number, evidenced in our results (see Figure 19). The HT-29 cells are genetically different from the pericryptal cells, which may cause a difference in optimal co-culture ratios. Future studies could compare HT-29 with pericryptal or patient-derived intestinal cells with stromal cells in co-culture.

4.2 IBD-modeling using our 3D co-culture system

Since the evaluation assay results showed that the 3D co-culture model maintains cell metabolic activity, cell viability, and cell proliferation, the next step was to assess the 3D model response to inflammatory and anti-inflammatory factors and thus simulate intestinal disease.

As mentioned in the "Methods" chapter, we used Lipopolysaccharide (LPS) to induce inflammation because of the technical ease and because LPS is involved in the pathway that leads to the transcription of pro-inflammatory cytokines, such as IL-1 β and TNF α .^{141,142} LPS was also chosen because of its high reproducibility compared to the other inflammatory factors. TNF α and IL-1 β cytokines were selected because they are clinically relevant and can be found in high concentrations in IBD patients¹⁴⁷. In addition, the secretion of these cytokines has also been studied for HT-29 cells.³⁷

The model response to inflammation and anti-inflammatory therapeutics was evaluated by measuring the above cytokine expression using the ELISA Assay. Both TNF α and IL-1 β concentrations were increased after adding LPS to the 3D models compared to control models. However, the absolute number of cytokine concentrations (pg/ml) in our epithelial-stromal cell model wasn't increased significantly. According to the literature, cytokine concentration is higher in the lamina propria and decreases the concentration gradient towards the intestinal epithelium.¹⁴⁷ However, when we calculated the percentage increase of cytokine expression compared to the control group, we saw that the difference between inflamed 3D and control models was significantly high for both TNF α and IL-1 β . Regarding TNF α expression, we noticed a considerable cytokine level increase when LPS was mixed with the culture medium (235.8% increase in cytokine expression) rather than when LPS was mixed with the 3D model (53.2% increase in cytokine expression). After reviewing the literature, a likely explanation was that LPS-binding protein in an FBS-containing medium helps LPS bind to Toll-like Receptor (TLR). This pathway triggers other inflammatory pathways and leads to the activation of TNF α transcription.¹⁵¹ Concerning the IL-1 β measurement, the 3D model inflammatory response was higher when LPS was mixed with the model (94.02% increase in cytokine expression) rather than when LPS was added to the culture medium (49.2% increase in cytokine expression).

Interesting results were reported after dexamethasone suppression of LPS-induced inflammation. In all cases, dexamethasone use in "inflamed" models decreased cytokine expression compared to the 3D co-culture systems containing only LPS. The estimated decrease percentages for TNF α and IL-1 β when dexamethasone was mixed with the LPS-model system were 41.1% and 29.54%, respectively. Moreover, when dexamethasone was added to the culture medium after a 2-hour model incubation with

LPS, the estimated decrease in TNF α and IL-1 β concentrations was 48.84% and 17.65%, respectively.

The ELISA Assay results support the hypothesis that the 3D co-culture model is responsive to inflammation and anti-inflammatory factors, indicating that our system could be used for drug screening. In the case of using patient-derived cells to generate 3D models, we could promote personalized medicine and therapeutic options focused on patient needs.

4.3 Limitations

The current study presents an innovative way for personalized medicine since 3D co-culture systems are tested for their response to inflammation and anti-inflammatory therapeutics. However, the study includes several limitations, and further studies are necessary.

First, the limited time during this master's project didn't allow the consecutive repetition of the experiments to improve some statistical parameters. However, the experiments were well organized, and the repetitive results in the future could establish the effectiveness of the 3D co-culture system.

In addition, another limitation of the study was the use of cell lines that have lost some of their host features after the repeatable passaging. Using primary colon organoids could recapitulate human colonic activity and disease.

Finally, our model doesn't include vascular cells. According to the literature, a crypt-pattern *in vitro* model has been generated, and it supports vascularization by combining stromal cells with vascular endothelium cells (3-cell type co-culture system).¹⁴⁷ So, our current avascular model doesn't simulate the human gut. However, there are opportunities to improve the 3D co-culture system.

CHAPTER 5

CONCLUSION & FUTURE APPROACH

In this master's thesis, we generated a 3D co-culture system of intestinal and fibroblast cells. We seeded the HT-29 cell line and the IRM-90 cell line in the Alginate-Gelatin Hydrogel. We proved that our 3D co-culture model supports cell metabolic activity, viability, and proliferation. Afterward, we designed IBD modeling using our 3D co-culture model. We showed that the LPS treatment to the "HT-29/IRM-90 3D co-culture hydrogel model" leads to increased levels of TNF α and IL-1 β cytokines compared to the control group. In addition, adding dexamethasone to the LPS-treated model leads to decreased cytokine levels. The final conclusion is that we generated a physiological bio-mimetic gut model responsive to inflammation and anti-inflammatory therapeutics. The future approach will generate a physiological bio-mimetic 3D gut model of IBD-patient-derived intestinal cells overlaid on a fibroblast basement membrane. Generating a gut-on-a-chip model using patient intestinal cells will simulate each patient's gut. Each individual's disease could be studied in detail, and the appropriate therapy could be chosen in advance for each patient.

BIBLIOGRAPHY

1. Guindi M, Riddell RH. Indeterminate colitis. *J Clin Pathol*. 2004;57(12):1233-1244.
2. Miehke S, Verhaegh B, Tontini GE, Madisch A, Langner C, Munch A. Microscopic colitis: pathophysiology and clinical management. *Lancet Gastroenterol Hepatol*. 2019;4(4):305-314.
3. Kaplan GG, Ng SC. Understanding and Preventing the Global Increase of Inflammatory Bowel Disease. *Gastroenterology*. 2017;152(2):313-321 e312.
4. Actis GC, Pellicano R, Fagoonee S, Ribaldone DG. History of Inflammatory Bowel Diseases. *J Clin Med*. 2019;8(11).
5. Mak WY, Zhao M, Ng SC, Burisch J. The epidemiology of inflammatory bowel disease: East meets west. *J Gastroenterol Hepatol*. 2020;35(3):380-389.
6. Molodecky NA, Soon IS, Rabi DM, et al. Increasing incidence and prevalence of the inflammatory bowel diseases with time, based on systematic review. *Gastroenterology*. 2012;142(1):46-54 e42; quiz e30.
7. Burisch J, Jess T, Martinato M, Lakatos PL, EpiCom E. The burden of inflammatory bowel disease in Europe. *J Crohns Colitis*. 2013;7(4):322-337.
8. Ng SC, Shi HY, Hamidi N, et al. Worldwide incidence and prevalence of inflammatory bowel disease in the 21st century: a systematic review of population-based studies. *Lancet*. 2017;390(10114):2769-2778.
9. Kappelman MD, Moore KR, Allen JK, Cook SF. Recent trends in the prevalence of Crohn's disease and ulcerative colitis in a commercially insured US population. *Dig Dis Sci*. 2013;58(2):519-525.
10. Coward S, Clement F, Benchimol EI, et al. Past and Future Burden of Inflammatory Bowel Diseases Based on Modeling of Population-Based Data. *Gastroenterology*. 2019;156(5):1345-1353 e1344.
11. Leddin D, Tamim H, Levy AR. Decreasing incidence of inflammatory bowel disease in eastern Canada: a population database study. *BMC Gastroenterol*. 2014;14:140.
12. Bitton A, Vutcovici M, Patenaude V, Sewitch M, Suissa S, Brassard P. Epidemiology of inflammatory bowel disease in Quebec: recent trends. *Inflamm Bowel Dis*. 2014;20(10):1770-1776.
13. Benchimol EI, Manuel DG, Guttman A, et al. Changing age demographics of inflammatory bowel disease in Ontario, Canada: a population-based cohort study of epidemiology trends. *Inflamm Bowel Dis*. 2014;20(10):1761-1769.
14. Kuenzig ME, Benchimol EI, Lee L, et al. The Impact of Inflammatory Bowel Disease in Canada 2018: Direct Costs and Health Services Utilization. *J Can Assoc Gastroenterol*. 2019;2(Suppl 1):S17-S33.
15. Kaplan GG, Ng SC. Globalisation of inflammatory bowel disease: perspectives from the evolution of inflammatory bowel disease in the UK and China. *Lancet Gastroenterol Hepatol*. 2016;1(4):307-316.
16. Windsor JW, Kaplan GG. Evolving Epidemiology of IBD. *Curr Gastroenterol Rep*. 2019;21(8):40.
17. Park J, Cheon JH. Incidence and Prevalence of Inflammatory Bowel Disease across Asia. *Yonsei Med J*. 2021;62(2):99-108.
18. Collaborators GBDIBD. The global, regional, and national burden of inflammatory bowel disease in 195 countries and territories, 1990-2017: a systematic analysis for the Global Burden of Disease Study 2017. *Lancet Gastroenterol Hepatol*. 2020;5(1):17-30.

19. Guan Q. A Comprehensive Review and Update on the Pathogenesis of Inflammatory Bowel Disease. *J Immunol Res*. 2019;2019:7247238.
20. Mirkov MU, Verstockt B, Cleynen I. Genetics of inflammatory bowel disease: beyond NOD2. *Lancet Gastroenterol Hepatol*. 2017;2(3):224-234.
21. Huang H, Fang M, Jostins L, et al. Fine-mapping inflammatory bowel disease loci to single-variant resolution. *Nature*. 2017;547(7662):173-178.
22. Yamamoto S, Ma X. Role of Nod2 in the development of Crohn's disease. *Microbes Infect*. 2009;11(12):912-918.
23. Cohen LJ, Cho JH, Gevers D, Chu H. Genetic Factors and the Intestinal Microbiome Guide Development of Microbe-Based Therapies for Inflammatory Bowel Diseases. *Gastroenterology*. 2019;156(8):2174-2189.
24. Nishida A, Inoue R, Inatomi O, Bamba S, Naito Y, Andoh A. Gut microbiota in the pathogenesis of inflammatory bowel disease. *Clin J Gastroenterol*. 2018;11(1):1-10.
25. Zuo T, Kamm MA, Colombel JF, Ng SC. Urbanization and the gut microbiota in health and inflammatory bowel disease. *Nat Rev Gastroenterol Hepatol*. 2018;15(7):440-452.
26. Rizzello F, Spisni E, Giovannardi E, et al. Implications of the Westernized Diet in the Onset and Progression of IBD. *Nutrients*. 2019;11(5).
27. Raoul P, Cintoni M, Palombaro M, et al. Food Additives, a Key Environmental Factor in the Development of IBD through Gut Dysbiosis. *Microorganisms*. 2022;10(1).
28. Knight-Sepulveda K, Kais S, Santaolalla R, Abreu MT. Diet and Inflammatory Bowel Disease. *Gastroenterol Hepatol (N Y)*. 2015;11(8):511-520.
29. Trakman GL, Lin WYY, Hamilton AL, et al. Processed Food as a Risk Factor for the Development and Perpetuation of Crohn's Disease-The ENIGMA Study. *Nutrients*. 2022;14(17).
30. Boyko EJ, Perera DR, Koepsell TD, Keane EM, Inui TS. Effects of cigarette smoking on the clinical course of ulcerative colitis. *Scand J Gastroenterol*. 1988;23(9):1147-1152.
31. Underner M, Perriot J, Cosnes J, Beau P, Peiffer G, Meurice JC. [Smoking, smoking cessation and Crohn's disease]. *Presse Med*. 2016;45(4 Pt 1):390-402.
32. Rozich JJ, Holmer A, Singh S. Effect of Lifestyle Factors on Outcomes in Patients With Inflammatory Bowel Diseases. *Am J Gastroenterol*. 2020;115(6):832-840.
33. AlQasrawi D, Qasem A, Naser SA. Divergent Effect of Cigarette Smoke on Innate Immunity in Inflammatory Bowel Disease: A Nicotine-Infection Interaction. *Int J Mol Sci*. 2020;21(16).
34. Strachan DP. Hay fever, hygiene, and household size. *BMJ*. 1989;299(6710):1259-1260.
35. Lee SH, Kwon JE, Cho ML. Immunological pathogenesis of inflammatory bowel disease. *Intest Res*. 2018;16(1):26-42.
36. Chalkidi N, Paraskeva C, Koliarakis V. Fibroblasts in intestinal homeostasis, damage, and repair. *Front Immunol*. 2022;13:924866.
37. Mahapatro M, Erkert L, Becker C. Cytokine-Mediated Crosstalk between Immune Cells and Epithelial Cells in the Gut. *Cells*. 2021;10(1).
38. Yamada A, Arakaki R, Saito M, Tsunematsu T, Kudo Y, Ishimaru N. Role of regulatory T cell in the pathogenesis of inflammatory bowel disease. *World J Gastroenterol*. 2016;22(7):2195-2205.
39. McGovern D, Powrie F. The IL23 axis plays a key role in the pathogenesis of IBD. *Gut*. 2007;56(10):1333-1336.
40. Coskun M. Intestinal epithelium in inflammatory bowel disease. *Front Med (Lausanne)*. 2014;1:24.
41. Li MC, He SH. IL-10 and its related cytokines for treatment of inflammatory bowel disease. *World J Gastroenterol*. 2004;10(5):620-625.
42. Leppkes M, Neurath MF. Cytokines in inflammatory bowel diseases - Update 2020. *Pharmacol Res*. 2020;158:104835.

43. Dinarello CA. Interleukin-1beta and the autoinflammatory diseases. *N Engl J Med*. 2009;360(23):2467-2470.
44. McAlindon ME, Hawkey CJ, Mahida YR. Expression of interleukin 1 beta and interleukin 1 beta converting enzyme by intestinal macrophages in health and inflammatory bowel disease. *Gut*. 1998;42(2):214-219.
45. Coccia M, Harrison OJ, Schiering C, et al. IL-1beta mediates chronic intestinal inflammation by promoting the accumulation of IL-17A secreting innate lymphoid cells and CD4(+) Th17 cells. *J Exp Med*. 2012;209(9):1595-1609.
46. Sanchez-Munoz F, Dominguez-Lopez A, Yamamoto-Furusho JK. Role of cytokines in inflammatory bowel disease. *World J Gastroenterol*. 2008;14(27):4280-4288.
47. Nemeth ZH, Bogdanovski DA, Barratt-Stopper P, Paglinco SR, Antonioli L, Rolandelli RH. Crohn's Disease and Ulcerative Colitis Show Unique Cytokine Profiles. *Cureus*. 2017;9(4):e1177.
48. Conrad K, Roggenbuck D, Laass MW. Diagnosis and classification of ulcerative colitis. *Autoimmun Rev*. 2014;13(4-5):463-466.
49. Gajendran M, Loganathan P, Catinella AP, Hashash JG. A comprehensive review and update on Crohn's disease. *Dis Mon*. 2018;64(2):20-57.
50. Sange AH, Srinivas N, Sarnaik MK, et al. Extra-Intestinal Manifestations of Inflammatory Bowel Disease. *Cureus*. 2021;13(8):e17187.
51. Bernstein CN, Blanchard JF, Rawsthorne P, Yu N. The prevalence of extraintestinal diseases in inflammatory bowel disease: a population-based study. *Am J Gastroenterol*. 2001;96(4):1116-1122.
52. Wils P, Caron B, D'Amico F, Danese S, Peyrin-Biroulet L. Abdominal Pain in Inflammatory Bowel Diseases: A Clinical Challenge. *J Clin Med*. 2022;11(15).
53. Lutgens MW, van Oijen MG, van der Heijden GJ, Vleggaar FP, Siersema PD, Oldenburg B. Declining risk of colorectal cancer in inflammatory bowel disease: an updated meta-analysis of population-based cohort studies. *Inflamm Bowel Dis*. 2013;19(4):789-799.
54. Wijnands AM, de Jong ME, Lutgens M, et al. Prognostic Factors for Advanced Colorectal Neoplasia in Inflammatory Bowel Disease: Systematic Review and Meta-analysis. *Gastroenterology*. 2021;160(5):1584-1598.
55. Greuter T, Vavricka S, Konig AO, Beaugerie L, Scharl M, Swiss Ibdnet aowgotSSoG. Malignancies in Inflammatory Bowel Disease. *Digestion*. 2020;101 Suppl 1:136-145.
56. Pedersen N, Duricova D, Elkjaer M, Gamborg M, Munkholm P, Jess T. Risk of extra-intestinal cancer in inflammatory bowel disease: meta-analysis of population-based cohort studies. *Am J Gastroenterol*. 2010;105(7):1480-1487.
57. Huang S, Li L, Ben-Horin S, et al. Mucosal Healing Is Associated With the Reduced Disabling Disease in Crohn's Disease. *Clin Transl Gastroenterol*. 2019;10(3):e00015.
58. Boal Carvalho P, Cotter J. Mucosal Healing in Ulcerative Colitis: A Comprehensive Review. *Drugs*. 2017;77(2):159-173.
59. Bryant RV, Winer S, Travis SP, Riddell RH. Systematic review: histological remission in inflammatory bowel disease. Is 'complete' remission the new treatment paradigm? An IOIBD initiative. *J Crohns Colitis*. 2014;8(12):1582-1597.
60. Bessissow T, Lemmens B, Ferrante M, et al. Prognostic value of serologic and histologic markers on clinical relapse in ulcerative colitis patients with mucosal healing. *Am J Gastroenterol*. 2012;107(11):1684-1692.
61. Rosenberg L, Nanda KS, Zenlea T, et al. Histologic markers of inflammation in patients with ulcerative colitis in clinical remission. *Clin Gastroenterol Hepatol*. 2013;11(8):991-996.
62. Colombel JF, D'Haens G, Lee WJ, Petersson J, Panaccione R. Outcomes and Strategies to Support a Treat-to-target Approach in Inflammatory Bowel Disease: A Systematic Review. *J Crohns Colitis*. 2020;14(2):254-266.

63. Cai Z, Wang S, Li J. Treatment of Inflammatory Bowel Disease: A Comprehensive Review. *Front Med (Lausanne)*. 2021;8:765474.
64. Punchard NA, Greenfield SM, Thompson RP. Mechanism of action of 5-aminosalicylic acid. *Mediators Inflamm*. 1992;1(3):151-165.
65. Oh-Oka K, Kojima Y, Uchida K, et al. Induction of Colonic Regulatory T Cells by Mesalamine by Activating the Aryl Hydrocarbon Receptor. *Cell Mol Gastroenterol Hepatol*. 2017;4(1):135-151.
66. Gisbert JP, Gonzalez-Lama Y, Mate J. 5-Aminosalicylates and renal function in inflammatory bowel disease: a systematic review. *Inflamm Bowel Dis*. 2007;13(5):629-638.
67. Hayashi R, Wada H, Ito K, Adcock IM. Effects of glucocorticoids on gene transcription. *Eur J Pharmacol*. 2004;500(1-3):51-62.
68. Ford AC, Bernstein CN, Khan KJ, et al. Glucocorticosteroid therapy in inflammatory bowel disease: systematic review and meta-analysis. *Am J Gastroenterol*. 2011;106(4):590-599; quiz 600.
69. Barrett K, Saxena S, Pollok R. Using corticosteroids appropriately in inflammatory bowel disease: a guide for primary care. *Br J Gen Pract*. 2018;68(675):497-498.
70. Buchman AL. Side effects of corticosteroid therapy. *J Clin Gastroenterol*. 2001;33(4):289-294.
71. Singh A, Mahajan R, Kedia S, et al. Use of thiopurines in inflammatory bowel disease: an update. *Intest Res*. 2022;20(1):11-30.
72. Jharap B, Seinen ML, de Boer NK, et al. Thiopurine therapy in inflammatory bowel disease patients: analyses of two 8-year intercept cohorts. *Inflamm Bowel Dis*. 2010;16(9):1541-1549.
73. Rusnak F, Mertz P. Calcineurin: form and function. *Physiol Rev*. 2000;80(4):1483-1521.
74. Levin AD, Wildenberg ME, van den Brink GR. Mechanism of Action of Anti-TNF Therapy in Inflammatory Bowel Disease. *J Crohns Colitis*. 2016;10(8):989-997.
75. Gerriets V, Goyal A, Khaddour K. Tumor Necrosis Factor Inhibitors. In: *StatPearls*. Treasure Island (FL)2022.
76. Ben-Horin S, Kopylov U, Chowers Y. Optimizing anti-TNF treatments in inflammatory bowel disease. *Autoimmun Rev*. 2014;13(1):24-30.
77. Parigi TL, Iacucci M, Ghosh S. Blockade of IL-23: What is in the Pipeline? *J Crohns Colitis*. 2022;16(Supplement_2):ii64-ii72.
78. Honap S, Meade S, Ibraheim H, Irving PM, Jones MP, Samaan MA. Effectiveness and Safety of Ustekinumab in Inflammatory Bowel Disease: A Systematic Review and Meta-Analysis. *Dig Dis Sci*. 2022;67(3):1018-1035.
79. Valenti M, Narcisi A, Pavia G, Gargiulo L, Costanzo A. What Can IBD Specialists Learn from IL-23 Trials in Dermatology? *J Crohns Colitis*. 2022;16(Supplement_2):ii20-ii29.
80. Gottlieb ZS, Sands BE. Personalised Medicine with IL-23 Blockers: Myth or Reality? *J Crohns Colitis*. 2022;16(Supplement_2):ii73-ii94.
81. Wang J, Macoritto M, Guay H, Davis JW, Levesque MC, Cao X. The Clinical Response of Upadacitinib and Risankizumab Is Associated With Reduced Inflammatory Bowel Disease Anti-TNF-alpha Inadequate Response Mechanisms. *Inflamm Bowel Dis*. 2022.
82. Luzentales-Simpson M, Pang YCF, Zhang A, Sousa JA, Sly LM. Vedolizumab: Potential Mechanisms of Action for Reducing Pathological Inflammation in Inflammatory Bowel Diseases. *Front Cell Dev Biol*. 2021;9:612830.
83. Wyant T, Fedyk E, Abhyankar B. An Overview of the Mechanism of Action of the Monoclonal Antibody Vedolizumab. *J Crohns Colitis*. 2016;10(12):1437-1444.
84. Onali S, Pugliese D, Caprioli FA, et al. An Objective Comparison of Vedolizumab and Ustekinumab Effectiveness in Crohn's Disease Patients' Failure to TNF-Alpha Inhibitors. *Am J Gastroenterol*. 2022;117(8):1279-1287.

85. Tran V, Shammass RM, Sauk JS, Padua D. Evaluating tofacitinib citrate in the treatment of moderate-to-severe active ulcerative colitis: design, development and positioning of therapy. *Clin Exp Gastroenterol*. 2019;12:179-191.
86. Pantavou K, Yiallourou AI, Piovani D, et al. Efficacy and safety of biologic agents and tofacitinib in moderate-to-severe ulcerative colitis: A systematic overview of meta-analyses. *United European Gastroenterol J*. 2019;7(10):1285-1303.
87. Sandborn WJ, Peyrin-Biroulet L, Quirk D, et al. Efficacy and Safety of Extended Induction With Tofacitinib for the Treatment of Ulcerative Colitis. *Clin Gastroenterol Hepatol*. 2022;20(8):1821-1830 e1823.
88. Sandborn WJ, Ghosh S, Panes J, et al. Efficacy of Upadacitinib in a Randomized Trial of Patients With Active Ulcerative Colitis. *Gastroenterology*. 2020;158(8):2139-2149 e2114.
89. Lowe SC, Sauk JS, Limketkai BN, Kwaan MR. Declining Rates of Surgery for Inflammatory Bowel Disease in the Era of Biologic Therapy. *J Gastrointest Surg*. 2021;25(1):211-219.
90. Lamb CA, Kennedy NA, Raine T, et al. British Society of Gastroenterology consensus guidelines on the management of inflammatory bowel disease in adults. *Gut*. 2019;68(Suppl 3):s1-s106.
91. Naganuma M, Yokoyama Y, Motoya S, et al. Efficacy of apheresis as maintenance therapy for patients with ulcerative colitis in an open-label prospective multicenter randomised controlled trial. *J Gastroenterol*. 2020;55(4):390-400.
92. Nagaishi K, Arimura Y, Fujimiya M. Stem cell therapy for inflammatory bowel disease. *J Gastroenterol*. 2015;50(3):280-286.
93. Sato T, Stange DE, Ferrante M, et al. Long-term expansion of epithelial organoids from human colon, adenoma, adenocarcinoma, and Barrett's epithelium. *Gastroenterology*. 2011;141(5):1762-1772.
94. Yui S, Nakamura T, Sato T, et al. Functional engraftment of colon epithelium expanded in vitro from a single adult Lgr5(+) stem cell. *Nat Med*. 2012;18(4):618-623.
95. Sugimoto S, Sato T. Organoid vs In Vivo Mouse Model: Which is Better Research Tool to Understand the Biologic Mechanisms of Intestinal Epithelium? *Cell Mol Gastroenterol Hepatol*. 2022;13(1):195-197.
96. Choudhary A, Ibdah JA. Animal models in today's translational medicine world. *Mo Med*. 2013;110(3):220-222.
97. Baydi Z, Limami Y, Khalki L, et al. An Update of Research Animal Models of Inflammatory Bowel Disease. *ScientificWorldJournal*. 2021;2021:7479540.
98. Scalise M, Marino F, Salerno L, et al. From Spheroids to Organoids: The Next Generation of Model Systems of Human Cardiac Regeneration in a Dish. *Int J Mol Sci*. 2021;22(24).
99. Habanjar O, Diab-Assaf M, Caldefie-Chezet F, Delort L. 3D Cell Culture Systems: Tumor Application, Advantages, and Disadvantages. *Int J Mol Sci*. 2021;22(22).
100. Liu Y, Chen YG. 2D- and 3D-Based Intestinal Stem Cell Cultures for Personalized Medicine. *Cells*. 2018;7(12).
101. Scott A, Rouch JD, Jabaji Z, et al. Long-term renewable human intestinal epithelial stem cells as monolayers: A potential for clinical use. *J Pediatr Surg*. 2016;51(6):995-1000.
102. Tong Z, Martyn K, Yang A, et al. Towards a defined ECM and small molecule based monolayer culture system for the expansion of mouse and human intestinal stem cells. *Biomaterials*. 2018;154:60-73.
103. Wang X, Yamamoto Y, Wilson LH, et al. Cloning and variation of ground state intestinal stem cells. *Nature*. 2015;522(7555):173-178.
104. Kapalczynska M, Kolenda T, Przybyla W, et al. 2D and 3D cell cultures - a comparison of different types of cancer cell cultures. *Arch Med Sci*. 2018;14(4):910-919.
105. Petersen OW, Ronnov-Jessen L, Howlett AR, Bissell MJ. Interaction with basement membrane serves to rapidly distinguish growth and differentiation pattern of normal and malignant human breast epithelial cells. *Proc Natl Acad Sci U S A*. 1992;89(19):9064-9068.

106. Fatehullah A, Tan SH, Barker N. Organoids as an in vitro model of human development and disease. *Nat Cell Biol.* 2016;18(3):246-254.
107. Chan BP, Leong KW. Scaffolding in tissue engineering: general approaches and tissue-specific considerations. *Eur Spine J.* 2008;17 Suppl 4(Suppl 4):467-479.
108. Langhans SA. Three-Dimensional in Vitro Cell Culture Models in Drug Discovery and Drug Repositioning. *Front Pharmacol.* 2018;9:6.
109. Caliri SR, Burdick JA. A practical guide to hydrogels for cell culture. *Nat Methods.* 2016;13(5):405-414.
110. Gunti S, Hoke ATK, Vu KP, London NR, Jr. Organoid and Spheroid Tumor Models: Techniques and Applications. *Cancers (Basel).* 2021;13(4).
111. Rosso F, Giordano A, Barbarisi M, Barbarisi A. From cell-ECM interactions to tissue engineering. *J Cell Physiol.* 2004;199(2):174-180.
112. Breslin S, O'Driscoll L. Three-dimensional cell culture: the missing link in drug discovery. *Drug Discov Today.* 2013;18(5-6):240-249.
113. Martinez-Maqueda D, Miralles B, Recio I. HT29 Cell Line. In: Verhoeckx K, Cotter P, Lopez-Exposito I, et al., eds. *The Impact of Food Bioactives on Health: in vitro and ex vivo models.* Cham (CH)2015:113-124.
114. Le Bivic A, Hirn M, Reggio H. HT-29 cells are an in vitro model for the generation of cell polarity in epithelia during embryonic differentiation. *Proc Natl Acad Sci U S A.* 1988;85(1):136-140.
115. Hartman KG, Bortner JD, Jr., Falk GW, et al. Modeling human gastrointestinal inflammatory diseases using microphysiological culture systems. *Exp Biol Med (Maywood).* 2014;239(9):1108-1123.
116. Cohen E, Ophir I, Shaul YB. Induced differentiation in HT29, a human colon adenocarcinoma cell line. *J Cell Sci.* 1999;112 (Pt 16):2657-2666.
117. Anzano MA, Rieman D, Prichett W, Bowen-Pope DF, Greig R. Growth factor production by human colon carcinoma cell lines. *Cancer Res.* 1989;49(11):2898-2904.
118. Forgue-Lafitte ME, Coudray AM, Breant B, Mester J. Proliferation of the human colon carcinoma cell line HT29: autocrine growth and deregulated expression of the c-myc oncogene. *Cancer Res.* 1989;49(23):6566-6571.
119. Ravikanth M, Soujanya P, Manjunath K, Saraswathi TR, Ramachandran CR. Heterogeneity of fibroblasts. *J Oral Maxillofac Pathol.* 2011;15(2):247-250.
120. Kendall RT, Feghali-Bostwick CA. Fibroblasts in fibrosis: novel roles and mediators. *Front Pharmacol.* 2014;5:123.
121. McKleroy W, Lee TH, Atabai K. Always cleave up your mess: targeting collagen degradation to treat tissue fibrosis. *Am J Physiol Lung Cell Mol Physiol.* 2013;304(11):L709-721.
122. Shaner NC. The mFruit collection of monomeric fluorescent proteins. *Clin Chem.* 2013;59(2):440-441.
123. Fages-Lartaud M, Tietze L, Elie F, Lale R, Hohmann-Marriott MF. mCherry contains a fluorescent protein isoform that interferes with its reporter function. *Front Bioeng Biotechnol.* 2022;10:892138.
124. Labowska MB, Cierluk K, Jankowska AM, Kulbacka J, Detyna J, Michalak I. A Review on the Adaption of Alginate-Gelatin Hydrogels for 3D Cultures and Bioprinting. *Materials (Basel).* 2021;14(4).
125. Lee KY, Mooney DJ. Alginate: properties and biomedical applications. *Prog Polym Sci.* 2012;37(1):106-126.
126. Engler AJ, Sen S, Sweeney HL, Discher DE. Matrix elasticity directs stem cell lineage specification. *Cell.* 2006;126(4):677-689.
127. Jiang T, Munguia-Lopez JG, Gu K, et al. Engineering bioprintable alginate/gelatin composite hydrogels with tunable mechanical and cell adhesive properties to modulate tumor spheroid growth kinetics. *Biofabrication.* 2019;12(1):015024.

128. Mikula K, Skrzypczak D, Ligas B, Witek-Krowiak A. Preparation of hydrogel composites using Ca²⁺ and Cu²⁺ ions as crosslinking agents. *SN Applied Sciences*. 2019;1(6):643.
129. Li X, Cao C, Yuan D, Liu Q, Zhao J. Effects of the Incorporation of Calcium Chloride on the Physical and Oxidative Stability of Filled Hydrogel Particles. *Foods*. 2022;11(3).
130. Rampersad SN. Multiple applications of Alamar Blue as an indicator of metabolic function and cellular health in cell viability bioassays. *Sensors (Basel)*. 2012;12(9):12347-12360.
131. Longhin EM, El Yamani N, Runden-Pran E, Dusinska M. The alamar blue assay in the context of safety testing of nanomaterials. *Front Toxicol*. 2022;4:981701.
132. Munshi S, Twining RC, Dahl R. Alamar blue reagent interacts with cell-culture media giving different fluorescence over time: potential for false positives. *J Pharmacol Toxicol Methods*. 2014;70(2):195-198.
133. Chassaing B, Aitken JD, Malleshappa M, Vijay-Kumar M. Dextran sulfate sodium (DSS)-induced colitis in mice. *Curr Protoc Immunol*. 2014;104:15 25 11-15 25 14.
134. Claes IJ, Lebeer S, Shen C, et al. Impact of lipoteichoic acid modification on the performance of the probiotic *Lactobacillus rhamnosus* GG in experimental colitis. *Clin Exp Immunol*. 2010;162(2):306-314.
135. Almutary AG, Alnuqaydan AM, Almatroodi SA, Bakshi HA, Chellappan DK, Tambuwala MM. Development of 3D-Bioprinted Colitis-Mimicking Model to Assess Epithelial Barrier Function Using Albumin Nano-Encapsulated Anti-Inflammatory Drugs. *Biomimetics (Basel)*. 2023;8(1).
136. Boirivant M, Fuss IJ, Chu A, Strober W. Oxazolone colitis: A murine model of T helper cell type 2 colitis treatable with antibodies to interleukin 4. *J Exp Med*. 1998;188(10):1929-1939.
137. Neurath M, Fuss I, Strober W. TNBS-colitis. *Int Rev Immunol*. 2000;19(1):51-62.
138. Antoniou E, Margonis GA, Angelou A, et al. The TNBS-induced colitis animal model: An overview. *Ann Med Surg (Lond)*. 2016;11:9-15.
139. Angrisano T, Pero R, Peluso S, et al. LPS-induced IL-8 activation in human intestinal epithelial cells is accompanied by specific histone H3 acetylation and methylation changes. *BMC Microbiol*. 2010;10:172.
140. De Gregorio A, Krasnowska EK, Zonfrillo M, et al. Influence of Polydatin on the Tumor Microenvironment In Vitro: Studies with a Colon Cancer Cell Model. *Int J Mol Sci*. 2022;23(15).
141. Molteni M, Gemma S, Rossetti C. The Role of Toll-Like Receptor 4 in Infectious and Noninfectious Inflammation. *Mediators Inflamm*. 2016;2016:6978936.
142. Lang CH, Silvis C, Deshpande N, Nystrom G, Frost RA. Endotoxin stimulates in vivo expression of inflammatory cytokines tumor necrosis factor alpha, interleukin-1beta, -6, and high-mobility-group protein-1 in skeletal muscle. *Shock*. 2003;19(6):538-546.
143. Beaurivage C, Kanapeckaitė A, Loomans C, Erdmann KS, Stallen J, Janssen RAJ. Development of a human primary gut-on-a-chip to model inflammatory processes. *Sci Rep*. 2020;10(1):21475.
144. Gewert K, Svensson U, Andersson K, Holst E, Sundler R. Dexamethasone differentially regulates cytokine transcription and translation in macrophages responding to bacteria or okadaic acid. *Cell Signal*. 1999;11(9):665-670.
145. Chuang TY, Cheng AJ, Chen IT, et al. Suppression of LPS-induced inflammatory responses by the hydroxyl groups of dexamethasone. *Oncotarget*. 2017;8(30):49735-49748.
146. Alhajj M, Farhana A. Enzyme Linked Immunosorbent Assay. In: *StatPearls*. Treasure Island (FL)2023.
147. Sotra A, Jozani KA, Zhang B. A vascularized crypt-patterned colon model for high-throughput drug screening and disease modelling. *Lab Chip*. 2023.
148. Creff J, Malaquin L, Besson A. In vitro models of intestinal epithelium: Toward bioengineered systems. *J Tissue Eng*. 2021;12:2041731420985202.
149. Radulescu DM, Neacsu IA, Grumezescu AM, Andronescu E. New Insights of Scaffolds Based on Hydrogels in Tissue Engineering. *Polymers (Basel)*. 2022;14(4).

150. Neal JV, Potten CS. Description and basic cell kinetics of the murine pericryptal fibroblast sheath. *Gut*. 1981;22(1):19-24.
151. Hoareau L, Bencharif K, Rondeau P, et al. Signaling pathways involved in LPS induced TNFalpha production in human adipocytes. *J Inflamm (Lond)*. 2010;7:1.